ABSTRACT

Title of dissertation: SIMULATIONS OF ACCRETION MECHANISMS
                           AND OBSERVATIONAL SIGNATURES OF
                           BLACK HOLE ACCRETION DISKS

                           Megan Smith
                           Doctor of Philosophy, 2019

Dissertation directed by: Professor Jonathan McKinney
                           Department of Physics

Black holes have been a subject of fascination since they were first theorized
about over a century ago. There are many questions about them left unanswered.
One of these is how matter is accreted onto these objects when the plasma around
them is rotating in an accretion disk. An answer to this question is likely to be found
in the magnetohydrodynamic processes that occur in the plasma, which require
highly sophisticated numerical simulations to explore. In this thesis, I describe an
analysis of one of the magnetohydrodynamic instabilities found in these simulations
as well as the observational signatures it produces, which might be recognized in
observations of these systems.

For the remainder of this thesis, I will discuss the formation and evolution
of a formal near-peer mentoring program for women in the University of Maryland
physics department. Mentoring programs have been shown to have a number of
benefits for both mentors and mentees. Primary among them is strengthening the
student's sense of belonging and science identity, which is linked to increased reten-

tion. Given the so-called "leaky pipeline" problem of women leaving physics, a field where they are already underrepresented, efforts to improve retention are vital and peer mentoring is one way to do this.

SIMULATIONS OF ACCRETION MECHANISMS AND OBSERVATIONAL SIGNATURES OF BLACK HOLE ACCRETION DISKS

by

Megan Smith

Dissertation submitted to the Faculty of the Graduate School of the
University of Maryland, College Park in partial fulfillment
of the requirements for the degree of
Doctor of Philosophy
2019

Advisory Committee:
Professor Jonathan McKinney, Co-Chair/Advisor
Professor Peter Shawhan, Co-Chair
Professor M. Coleman Miller
Professor James Drake
Professor Steven Rolston

Preface

Two of the body chapters of this dissertation are papers in various stages of publication.

Chapter 2 of this dissertation is published as Marshall, Avara, and McKinney (2018) [1] and is included here in its publish form with minor revisions. I carried out the writing of this paper and the analysis it contains, under the supervision of Professor Jonathan McKinney with assistance from Dr. Mark Avara. The work in Chapter 3 was carried out by me with assistance from Dr. Roman Gold and will be prepared for publication.

Acknowledgments

I would to thank the countless people who supported me and helped make this thesis possible. Without the encouragement of my family, friends, colleagues, and many others, this work would not exist.

First, I would like to thank my advisor, Jonathan McKinney, for his guidance and support throughout my time in grad school. I also want to thank the other members of my committee: Peter Shawhan, James Drake, Cole Miller, and Steve Rolston. I am also grateful for the support from the other members of our research group, Peter Polko, Roman Gold, Jane Dai, and Mark Avara, for helpful conversations, advice, and friendship.

During my time in grad school, I have gained some wonderful friends. Thank you to the friends who helped me make it through our first year, both academically and socially: Joe Garrett, George Hine, Kevin Pedro, and especially Nat Steinsultz, who forced me to develop a deeper appreciation for 80s music. To John Biddle and Jack Hellerstedt, for always hanging out in the grad lounge and passing along your wisdom to us first years. Through my involvement in Women in Physics, I met and worked with so many amazing people: Michelle Groce, Kristen Burson (who always seems to have a mentoring program for me to run in her absence), Rachel Lee, Deborah Hemingway, Hilary Hurst, Holly Tinkey, Liz Friedman, Monica Gutierrez, Batoul Banihashemi, Sarah Monk, Donna Hammer, Sonali Shukla, and Jessica Crosby. I have mentored several younger women during my time in graduate school, both formally and informally, all of whom have supported me just as much as

Darius, Doug, Jackie, Austin, Brynlee, and Corbyn for all of your support. I especially want to thank my grandma Sue for helping me furnish my apartment and my uncle Doug for making sure I always had more chicken than I knew what to do with, feeding not just me but also many of my grad school friends. To my cousin Jackie - you might have graduated before me, but I still have more degrees than you! To Susan for always accepting and caring for me. To Mary for always doing whatever you could to celebrate with me and make me feel included in the family even though I was across the country. Thank you to Alex for being a wonderful little brother and making me feel wise when grad school did the opposite by asking for my advice and opinion, even if it was just how I thought the Red Wings would do that year.

Thank you to my dad for encouraging me in my scientific pursuits, from taking me to see Star Wars for the first time to getting optics catalogs to better connect with my research. Thank you so, so much to my mom, who has done and continues to do more for me than I can possibly say, including late nights of stargazing and suggesting I go to grad school in the first place.

I also want to acknowledge the Smith family. While I have only recently joined the family, you have given me so much advice, encouragement, and support in that time.

Most importantly, thank you to my husband, Zach. You believed in me even when I didn't and I wouldn't have finished this without your encouragement and help.

Table of Contents

List of Figures

List of Abbreviations

AGN	Active Galactic Nucleus
AGN	Astronomy Gentleladies' Network
APS	American Physical Society
BH	Black hole
EHT	Event Horizon Telescope
GR	General Relativity
IAU	Internatioal Astronomical Union
IEEE	Institute of Electrical and Electronic Engineers
ISCO	Innermost stable circular orbit
MHD	Magnetohydrodynamics
MRI	Magnetorotational instability
RT	Rayleigh-Taylor
SMBH	Supermassive black hole
STEM	Science, Technology, Engineering, and Mathematics
VLBI	Very long baseline interferometry
WiP	Women in Physics

Chapter 1: Introduction

Black holes (BH) are a subject of fascination for astronomers and have been
since Schwarzschild first calculated his solution [2] to Einstein's field equations [3]
over a century ago. Everything from their very existence to what is beyond the
event horizon to how they form and grow has been debated and studied by both
observers and theorists. One area that links the two groups of scientists is the
intense luminosity seen at the center of galaxies. Observers have studied the exotic
objects that produce this radiation at many different wavelengths and used their
observations to constrain the size of the central object, pointing to the light being
emitted by matter falling onto a supermassive black hole (SMBH) ($M > 10^6 M_\odot$)
[4, 5]. The exact details of how the matter accretes onto an SMBH cannot be
determined from observations at this time, so sophisticated simulations are studied
in their place, though the Event Horizon Telescope (EHT) is now beginning to probe
this phenomenon using very long baseline interferometry (VLBI). Also of interest
in these systems are the relativistic jets and bursts of particles originating from
these same central regions. In this dissertation, I will describe the study of the
magnetic Rayleigh-Taylor instability in a SMBH accretion disk and its impact on
the mass inflow onto the BH using one such simulations, as well as the observational

signatures that this instability produces, connecting back to observations. Below I present a brief overview of the current understanding of BH accretion mechanisms, then discuss the numerical methods used in the simulations that I studied.

1.1 Active Galactic Nuclei Observations

For many decades, observers have identified objects with very high luminosities, known as Active Galactic Nuclei, along with other historical names. These objects emit much higher emission than that produced by the nuclear processes fueling stars, with the emission spanning the electromagnetic spectrum. Seyfert first identified galaxies with strong emission in 1943 [6]. One of these galaxies (NGC 1275) was included in Baade and Minkowski's study of radio sources, where they compared it to Cygnus A, one of the strongest observed radio emitters, bringing more attention to these exotic objects [7]. A few years after this, Woltjer showed that these objects must be both massive and confined to a small angular size [8]. Shortly after this paper, Schmidt discovered the first quasar [9], or quasi-stellar object, the most luminous type of AGN. A year later, Zeldovich and Salpeter independently suggested that quasars were powered by accretion onto SMBHs [10, 11].

While these observations were given many different names historically (e.g. Seyfert galaxy, quasar, blazar, etc. [4, 5]), this is due to variation in a small set of parameters (e.g. viewing angle, mass and spin of the central object, mass accretion rate of the system, etc.) rather than fundamental differences of the physical objects themselves. These objects are identified by certain features, such as very small

emitting regions (~ 1 mpc $\sim 3 \times 10^7$ km), high luminosity (up to 10^{48} erg s^{-1}), and broad-band continuum emission [4, 5], though not all subcategories display all of these properties. Many AGN also exhibit luminosity variability, particularly in the optical band, and weak polarization [4].

1.2 Accretion in Astrophysics

Accretion is the process where matter in a gravitational potential is pulled onto the central object, increasing the mass of that object. In astrophysics, accretion is divided into two regimes, depending on the angular momentum of the matter surrounding the central object. When this accreting matter, predominantly gas or plasma, but which might include dust grains or other solids, has low angular momentum, it is in the Bondi regime, where it plunges into the central object. In the simplest case, the matter has no angular momentum and falls directly onto the central object at a rate determined by just the mass of the object and the speed of sound in the gas [12]. This regime is useful for defining a characteristic luminosity, found by balancing the inward gravitational force with the outward radiative force of fully ionized hydrogen undergoing spherically symmetric accretion, known as the Eddington luminosity,

$$L_E = \frac{4\pi cGM}{\kappa} \approx 1.25 \times 10^{38} \frac{M}{M_\odot} \text{erg s}^{-1}, \qquad (1.1)$$

where c is the speed of light, G is the gravitational constant, M is the mass of the central object, $\kappa = 0.4 \text{cm}^2 \text{g}^{-1}$ is the opacity of Thompson scattering, and $M_\odot$ is the

mass of the Sun. The luminosity can also be written as a function of the accretion rate, $\dot{M}$,

$$L = \eta \dot{M} c^2, \tag{1.2}$$

where η is the radiative efficiency. From this, a scale for the rate of accretion can be found,

$$\dot{M}_E = \frac{L_E}{\eta c^2} \approx 1.4 \times 10^{18} \frac{M}{M_\odot} \mathrm{g\,s^{-1}}, \tag{1.3}$$

for a value of $\eta \approx 0.1$. This value can be used to separate different subcategories of accretion regimes.

While this regime has provided a useful reference point for understanding accretion, gas with low enough angular momentum per unit mass to be in this category is uncommon in astrophysical environments. Also, Bondi accretion does not consider the effects of radiative transfer, further limiting its usefulness [13].

The second accretion regime occurs when the specific angular momentum of the gas is high relative to GM/c. Due to conservation of angular momentum, this matter cannot fall directly onto the central object, but will orbit it at the radius where the centrifugal force is comparable to the gravitational force, forming an accretion disk. Only when angular momentum is transported away from the gas can it accrete onto the central object, dissipating energy through some form of turbulence as it does so. The mechanisms by which energy is dissipated and angular momentum is transported out of the disk further divides this regime.

Efficient radiation of energy in an accretion flow will lead to a geometrically thin, optically thick disk known as the α-disk model from Shakura and Sunyaev [14],

in which α characterizes the transport of angular momentum in the disk. Specifically, they propose a viscosity

$$\nu = \alpha c_s H, \tag{1.4}$$

where c_s is the speed of sound in the plasma and H is the scale height of the disk. Intuitively, this formulation makes sense, as eddies created by the turbulence driving angular momentum transport would be limited by the fundamental properties of the disk.

Novikov and Thorne [15] use the same form to characterize their thin disk model. While Shakura and Sunyaev neglected the spin of the SMBH in their treatment of accretion, Novikov and Thorne extend this model to the Kerr metric, the solution to the Einstein field equations for a rotating BH [16, 17]. This model, while simple, has been the foundation of accretion disk theory since it was developed. It has been particularly successful modeling luminous AGN and X-ray binaries (XRBs) in the thermal state of their outburst cycle [18, 19].

On the other hand, there are also models with radiatively inefficient accretion flows (RIAF), which can again be divided into different cases based on the accretion rate. For $\dot{M} \gtrsim \dot{M}_E$, the disk falls into the slim disk model, characterized by an optically thick gas and cold accretion flow [20, 21]. This model has been used to study systems like ultraluminous X-ray sources [22, 23]. For very low accretion rates ($\dot{M} \lesssim 10^{-2}\dot{M}_E$), the disk becomes optically thin and geometrically thick, with a hot accretion flow [24]. This type of model includes the advection-dominated accretion flow (ADAF), which has been used to model the accretion of Sgr A* [25, 26] and

other low-luminosity AGNs [27].

1.3 Magnetic Fields in Accretion Disk Plasma

1.3.1 Ideal Magnetohydrodynamics

While the previous discussion has largely neglected how magnetic fields affect accretion, focusing on angular momentum and energy, they are part of the turbulence-driving viscosity found in the α-disk model. To include them, consider the simplest treatment of the plasma-magnetic field interaction: ideal magnetohydrodynamics (MHD). The equations that govern ideal MHD are

$$\frac{\partial \rho}{\partial t} + \nabla \cdot [\rho \mathbf{v}] = 0, \tag{1.5}$$

$$\frac{\partial \rho \mathbf{v}}{\partial t} + \nabla \cdot [\rho \mathbf{v}\mathbf{v} - \mathbf{B}\mathbf{B} + \mathbf{P}] = 0, \tag{1.6}$$

$$\frac{\partial E}{\partial t} + \nabla \cdot [(E + P)\mathbf{v} - \mathbf{B}(\mathbf{B} \cdot \mathbf{v})] = 0, \tag{1.7}$$

$$\frac{\partial \mathbf{B}}{\partial t} - \nabla \times [\mathbf{v} \times \mathbf{B}] = 0, \tag{1.8}$$

where $\mathbf{P}$ is the pressure tensor with components $P = P_{gas} + B^2/2$,

$$E = \frac{P_{gas}}{\Gamma - 1} + \frac{1}{2}\rho v^2 + \frac{B^2}{2} \tag{1.9}$$

is the total energy density, and $B^2 = \mathbf{B} \cdot \mathbf{B}$. To close this set of equations, the ideal gas pressure, $P_{gas} = (\Gamma - 1)u_g$, where Γ is the ratio of specific heats and u_g is the

internal energy density, is used.

The equations above are the non-relativistic conservation of rest mass (Eqn. 1.5), momentum (Eqn. 1.6), and energy (Eqn. 1.7) equations and the induction equation (Eqn. 1.8), derived from Faraday's law and the ideal Ohm's law equations. In this form, these equations represent a plasma with no source terms in a Minkowski spacetime, not the more complex version solved in BH accretion disk simulations, but are more familiar to most and therefore better for developing an intuitive understanding of the environment. The relativistic versions used in the simulations can be found in Gammie et al. [28], specifically their equations 2 (conservation of particle number), 4 (four energy-momentum equation using the MHD stress-energy tensor found in equation 11), and 18 (the induction equation, which is subject to equation 19).

1.3.2   Magnetorotational Instability

A breakthrough in disk theory was made in 1991 when Balbus and Hawley [29, 30] showed that the magnetorotational instability (MRI), an MHD instability that arises in weakly magnetized plasma, leads to a turbulent viscosity, which is necessary as the shear viscosity does not generate enough angular momentum transport when compared with observations. This instability was first studied by Velikhov [31] and Chandrasekhar [32] and agrees with the suggestion in Shakura and Sunyaev [14] that magnetic turbulence drove angular momentum transport.

In its simplest form, the MRI occurs in an environment with a magnetic field

oriented along a given axis (e.g. $\hat{z}$) with a perturbation along an orthogonal axis (e.g. $\hat{r}$) in the presence of a shear along the third axis (e.g. $\hat{\phi}$). These conditions are easily satisfied by a differential rotating accretion disk. To develop an intuitive understanding of this process, consider the following mechanical model from Balbus and Hawley's 1998 review [30]. Two point masses, m_{inner} at radius r_{inner} and m_{outer} at radius r_{outer}, are connected by a weak, massless spring, representing the weak magnetic field. While they are initially close, as these masses rotate at their different radii, they are separated further by the more rapid rotation of m_{inner}. This separation stretches the spring, creating a small restoring force, transferring angular momentum from m_{inner} to m_{outer}. This causes m_{inner} to fall to an even smaller radius and m_{outer} to move to a larger radius, which stretches the spring even more, increasing the force on the masses, and creating a run away process.

More formally, a dispersion relation can be derived by considering a small displacement $\xi = (\xi_r, \xi_\phi, 0)$ with a spatial and temporal dependence $e^{i(kz - \omega t)}$ in the equatorial plane of a disk with a weak vertical ($\hat{z}$) magnetic field and following the procedure outlined in Balbus and Hawley [33]. This leads to a perturbation in the magnetic field

$$\delta \mathbf{B} = \nabla \times (\xi \times \mathbf{B}) = ikB\xi. \tag{1.10}$$

Moving to a frame rotating with angular velocity Ω necessitates adding Coriolis and centrifugal forces to the equation of motion. The centrifugal force almost balances the radial gravitational force, leaving a residual force. The equations of motion are

then

$$\frac{d^2\xi_r}{dt^2} - 2\Omega\frac{d\xi_\phi}{dt} = -\left[(kv_A)^2 + \frac{d\Omega^2}{d\ln r}\right]\xi_r, \qquad (1.11)$$

$$\frac{d^2\xi_\phi}{dt^2} + 2\Omega\frac{d\xi_r}{dt} = -(kv_A)^2\xi_r. \qquad (1.12)$$

These lead to a dispersion relation of

$$\omega^4 - \omega^2\left[\kappa^2 + 2(kv_A)^2\right] + (kv_A)^2\left[(kv_A)^2 + \frac{d\Omega^2}{d\ln r}\right] = 0, \qquad (1.13)$$

where $v_A = B/\sqrt{4\pi\rho}$ is the Alfven speed and κ is the epicyclic frequency

$$\kappa^2 = 4\Omega^2 + \frac{d\Omega^2}{d\ln r} = \frac{1}{r^3}\frac{d(r^4\Omega^2)}{dr}. \qquad (1.14)$$

The MRI is unstable if

$$\frac{d\Omega^2}{d\ln r} < 0 \qquad (1.15)$$

and the maximum growth rate is

$$|\omega_{max}| = \frac{1}{2}\left|\frac{d\Omega^2}{d\ln r}\right|, \qquad (1.16)$$

which is 0.75Ω in a Keplerian disk, meaning the MRI operates on a suborbital time scale, rapidly amplifying the magnetic field.

An issue with the MRI turbulent disk model is that of the magnetic field structure. First, many SMBH systems have been found to have large scale ordered fields [34, 35, 36], rather than the weaker fields generated by the MRI. Second, the

MRI-generated field does not sustain relativistic jets [37, 38], a key component of SMBH accretion systems that astronomers seek to understand through simulations. These issues show that a different field topology is needed to better explain these phenomena. One alternative structure is a disk with a strong poloidal field built up on the BH [39, 40], known as the 'magnetically arrested disk' (MAD). However, the MRI is suppressed in simulations with such strong fields [40, 41]. This agrees with the analogy presented above, for a strong spring would lead to the oscillation of the masses, rather than the stretching leading to the run away process [30]. This means another generator of turbulence must be present. One possibility, the magnetic Rayleigh-Taylor (RT) instability is the focus of the next chapter and a description of it is given in the next section.

1.3.3   Magnetic Rayleigh-Taylor Instability

The magnetic RT instability was suggested as a possible driver of turbulence leading to angular momentum transport and accretion several decades ago by Elsner and Lamb [42, 43] and Arons and Lea [44], Arons and Lea [45], who focused on neutron star accretion. This instability has been studied in thin accretion disk simulations by many since then [46, 47, 48]. In particular, Li and Narayan [49] studied the magnetic RT instability at the interface of a high density, weakly magnetized accretion disk and a low density, strongly magnetized magnetosphere around a compact central object, applicable to either a neutron star or BH, depending on the angular velocity profile.

The magnetic RT instability occurs in an environment where a high density fluid is suspended against gravity over a lower density fluid with a magnetic field oriented parallel to the interface. If this interface is perturbed, the system will move toward a lower potential energy state as regions, or "fingers", of high density fluid push downwards into the lower density fluid, which will move upwards in so-called "bubbles" at the same time.

To understand the instability in an accretion disk, we follow the derivation presented in Li and Narayan [49]. Consider linear perturbations to the density gas pressure, velocity, and magnetic field in the disk plane

$$\begin{Bmatrix} \delta\rho \\ \delta p \\ \delta\mathbf{v} \\ \delta\mathbf{B} \end{Bmatrix} = \begin{Bmatrix} \rho_1(r) \\ p_1(r) \\ u(r)\hat{r} + v(r)\hat{\phi} \\ B_1(r)\hat{z} \end{Bmatrix} e^{i(k\phi - \omega t)}. \tag{1.17}$$

Assuming an incompressible fluid and neglecting resistivity and viscosity, to first order, the following wave equation is found

$$\frac{1}{r\rho_0}\frac{d}{dr}\left(r\rho_0\frac{d(ru)}{dr}\right) - \frac{k^2}{r^2}\left[\frac{\Omega_{eff}^2}{(\omega - k\Omega)^2}\frac{d\ln\rho_0}{d\ln r} - \frac{2\xi}{k(\omega - k\Omega)}\frac{d(\ln\rho_0\xi)}{d\ln r} + 1\right]ru = 0, \tag{1.18}$$

where

$$\Omega_{eff}^2 = -\frac{1}{r\rho_0}\frac{dp_{t,0}}{dr} \tag{1.19}$$

11

is the effective angular velocity and

$$\xi = \frac{1}{2r}\frac{d}{dr}(r^2\Omega) \tag{1.20}$$

is the vorticity frequency. For a system with a continuous angular momentum profile, such as a BH, $\Omega(r) = \Omega_m(r/r_m)^{-q}$, where Ω_m is the angular velocity at the interface and q is the index, which ranges from 0 to 2 in Li and Narayan [49], but realistically is more likely to be from 3/2 (Keplerian) to 2. ω will be an eigenvalue of Eqn. 1.18 and frequencies with $Im(\omega) > 0$ are unstable. They also find a more rigorous stability condition

$$-\left(\frac{\Omega_{eff}}{\Omega}\right)^2\left(\frac{d\ln\Omega}{d\ln r}\right)^{-2}\frac{d\ln\rho_0}{d\ln r} < \frac{1}{4}, \tag{1.21}$$

but do not consider it for their paper, finding the less formal condition sufficient for their work.

This instability is seen frequently in MAD simulations, as the innermost regions of the accretion disk create the appropriate environment for it to develop. My graduate studies have focused on how it affects the accretion rate of a thin MAD, described in more detail below, using both qualitative and quantitative methods. I then set out to find the effects the magnetic RT instability have on observations of SMBHs, as might be found by the EHT. These ideas are discussed in the next two chapters.

1.4 Numerical Simulations of Accretion Disks

Since it has only recently become possible to observe the innermost regions close to the BH in SMBH accretion disk systems, as only the EHT has the resolution and sensitivity to image structures on the scale of a few r_g and even it cannot yet probe the smallest interactions leading to MHD turbulence, many numerical methods were developed to understand the underlying physics, improving as technology allowed for more detailed simulations. These simulations were then linked to observations by the EHT and other telescopes through ray tracing and radiative transfer schemes, simulating observations of the modeled systems. Here I will discuss the particular methods used in my work presented in this dissertation, HARM [28, 38, 40] and ASTRORAY [50, 51, 52, 53]. For a more complete review of numerical techniques used in astrophysics, see Font's Living Review [54].

1.4.1 HARM

HARM, or High Accuracy Relativistic Magnetohydrodynamics, is a general relativistic (GR) MHD integrator. The first such code was created by Wilson in 1977 [55], who solved the GRMHD equations in the Kerr metric, but these techniques were not strongly pursued until the MRI was re-discovered by Balbus and Hawley [29] and the importance of magnetic fields in accretion disks was revealed. HARM uses a finite-volume method, where quantities are volume-averaged over grid cells and the flux between cells is computed, allowing the volume integrated quantities to be conserved to machine precision. HARM employs a conservative scheme rather

than a non-conservative one, which integrates the internal energy instead of the total energy. In addition to greater accuracy, conservative schemes that are total variation stable are guaranteed to converge to a weak solution of the equations in one dimension [56, 57], which is a good place to start even for multidimensional flows. The conserved quantities updated at each timestep in HARM are

$$\mathbf{U} \equiv \sqrt{-g}(\rho u^t, T^t_t, T^t_i, B^i), \tag{1.22}$$

where u^μ is the four-velocity, T^μ_ν is the stress-energy tensor, and B^i is the magnetic field three-vector. These quantities are updated with fluxes $\mathbf{F}$. A vector of "primitive" variables is also needed. These are

$$\mathbf{P} = (\rho, u, v^i, B^i), \tag{1.23}$$

where u is the internal energy and $v^i = u^i/u^t$ is the 3-velocity. These quantities are interpolated to model the flow within zones.

Both $\mathbf{U}$ and $\mathbf{P}$ are used within the code, but $\mathbf{P}$ is not updated directly. Instead, $\mathbf{P}(\mathbf{U})$ is found at the end of each timestep using a Newton-Raphson routine [13, 58]. Originally, $\mathbf{F}$ was evaluated using a MUSCL scheme with the "HLL" approach [59], but more advanced forms are used for the work presented here.

To preserve $\nabla \cdot \mathbf{B} = 0$, zone centered (or flux-interpolated) constrained transport [60] is used. In this method, $\mathbf{F}$ is evaluated at the grid cell edges, which are used to updated the fluxes at the cell center, smoothing them and ensuring $\nabla \cdot \mathbf{B} = 0$.

1.4.2 ASTRORAY

ASTRORAY [50] is a GR polarized radiative transfer code that can be applied to the output of GRMHD simulations like the HARM code described above. It models synchrotron emissivities, absorptivities, Faraday rotation and conversion from low luminosity AGNs and jets, using a thermal isotropic distribution function for electrons. The governing equation for nonrelativistic radiative transfer is

$$\frac{d\mathbf{S}}{ds} = \begin{pmatrix} \epsilon_I \\ \epsilon_Q \\ 0 \\ \epsilon_V \end{pmatrix} - \begin{pmatrix} \eta_I & \eta_Q & 0 & \eta_V \\ \eta_Q & \eta_I & \rho_V & 0 \\ 0 & -\rho_V & \eta_I & \rho_Q \\ \eta_V & 0 & -\rho_Q & \eta_I \end{pmatrix} \mathbf{S}, \tag{1.24}$$

where $\mathbf{S} = (I, Q, U, V)^T$ is the polarization vector where the components are the Stokes' parameters, ϵ_i are the emission coefficients,

$$\eta_I = \text{Im}(\alpha^{22} + \alpha^{11})/\nu, \tag{1.25}$$

$$\eta_Q = \text{Im}(\alpha^{11} - \alpha^{22})/\nu, \tag{1.26}$$

$$\eta_V = 2\text{Re}(\alpha^{12})/\nu, \tag{1.27}$$

$$\tag{1.28}$$

are the absorption coefficients,

$$\rho_V = 2\text{Im}(\alpha^{12})/\nu, \tag{1.29}$$

is the Faraday rotation coefficient,

$$\rho_Q = \text{Re}(\alpha^{22} - \alpha^{11})/\nu, \tag{1.30}$$

is the Faraday conversion coefficient, $\nu = \omega/2\pi$, and α^{ij} is the 4×4 response tensor derived for thermal physics. This is then extended to GR in a locally-flat co-moving frame by generalizing $\mathbf{S}$ to a set of photon occupation numbers $\mathbf{N} = \mathbf{S}/\nu^3$.

The code traces a uniform grid of geodesics from the image plane to the SMBH and integrates the intensity of the fluxes along them back to the image plane. To account for the evolution of the model as the light propagates, a number of data files before and after the current time are included in the calculation to simulate the spectra. This allows the user to select a set of files large enough to accurately generate the spectrum without needing to include the full simulation time, which would be too time-consuming.

1.4.3 Thin MAD Model

The work presented in Chapters 2 and 3 was done using the MADiHR simulation, a GRMHD model of a thin (ratio of half-height H to radius R, $H/R \approx 0.1$) MAD around a moderately rotating BH (a/M = 0.5) from Avara et al. [41]. This model was initially in a near-MAD state and becomes MAD out to a large radius as magnetic flux is advected inwards throughout the duration of the simulation.

The initial state was Keplerian with a rest-mass density profile that was Gaussian in angle and $\rho \propto r^{-0.6}$. Close to the innermost stable circular orbit

(ISCO), the density is tapered and the disk is truncated at r_{ISCO}. In the corona, $\rho = 10^{-4}(r/r_g)^{-3/2}$, where $r_g = GM/c^2$. The disk is expected to be radiation pressure dominated, so the adiabatic index $\Gamma = 4/3$ is chosen.

The magnetic field is initially polodial with a nearly-MAD flux (plasma beta $\beta = P_{gas}/P_b = 50$) inside $r = 30r_g$ and weaker sub-MAD flux ($\beta = 200$) outside this transition radius.

An ad hoc cooling function and temperature ceiling were implemented to keep the disk close to $H/R \approx 0.1$. See section 2.3 of Avara et al. [41] for full details.

The simulation has a resolution of $N_r \times N_\theta \times N_\phi = 192 \times 96 \times 208$. The radial grid spans from $R_{in} = 0.75r_H$ (where r_H is the horizon radius) to $R_{out} = 10^4 r_g$. The θ grid ranges from 0 to π. The radial and θ grids are similar to the mapping used in McKinney et al. [40], except for a smooth arctan transition from exponential to hyper-exponential radial grid spacing and $\eta_{jet} = 0$ for the θ grid spacing. The ϕ grid is equally spaced, ranging from 0 to 2π, with periodic boundary conditions. The radial boundary conditions are identical to McKinney et al. [40] and the polar boundary conditions are transmissive.

1.5 Near-Peer Mentoring

I have also spent much of my time as a doctoral student organizing and running a formal near-peer mentoring program through the University of Maryland (UMD) Women in Physics (WiP) group. After participating as a mentor in the first semester of the program's existence and gaining many benefits from it, I became the official

WiP mentoring coordinator. In the five years since, I have expanded the program and adapted the original components to better support the women participating in the program, both the graduate student mentors and undergraduate student mentees. These programs have many benefits, chief among them improved retention rates, which are important in fields such as physics where the percentage of women earning bachelor's degrees has stagnated at 20% [61].

1.6   Structure of the Dissertation

Accretion in astrophysical environments has many complexities that cannot be fully understood with today's telescopes, so simulations made using sophisticated codes such as those described above are vital to understanding these processes.

In chapter 2, I perform an analysis of the effects of the magnetic Rayleigh-Taylor instability in a thin MAD simulation. This includes the use of a three-dimensional visualization technique that I developed to better understand the evolution of the magnetic field structure during the magnetic Rayleigh-Taylor eruption.

Chapter 3 examines the observational signature of the same magnetic Rayleigh-Taylor event seen in chapter 2 and the relationship between the variations of the magnetic field on the black hole horizon and observed AGN variability.

Chapter 4 describes the structure of the WiP formal near-peer mentoring program, including a review of the relevant literature to examine the benefits that similar programs provide to the participants.

Chapter 2: Accretion Mechanisms in Thin MADs

2.1   Abstract

In accretion disks with large-scale ordered magnetic fields, the magnetorotational instability (MRI) is marginally suppressed, so other processes may drive angular momentum transport leading to accretion. Accretion could then be driven by large-scale magnetic fields via magnetic braking, and large-scale magnetic flux can build-up onto the black hole and within the disk leading to a magnetically-arrested disk (MAD). Such a MAD state is unstable to the magnetic Rayleigh-Taylor (RT) instability, which itself leads to vigorous turbulence and the emergence of low-density highly-magnetized bubbles. This instability was studied in a thin (ratio of half-height H to radius R, $H/R \approx 0.1$) MAD simulation, where it has a more dramatic effect on the dynamics of the disk than for thicker disks. Large amounts of flux are pushed off the black hole into the disk, leading to temporary decreases in stress, then this flux is reprocessed as the stress increases again. Throughout this process, we find that the dominant component of the stress is due to turbulent magnetic fields, despite the suppression of the axisymmetric MRI and the dominant presence of large-scale magnetic fields. This suggests that the magnetic RT instability plays a significant role in driving angular momentum transport in MADs.

2.2   Introduction

Accretion disks are a central focus of interest in high energy astrophysics. From observations of AGN and similar objects, it is known that matter is flowing onto the central black hole (BH) of the system due to the release of intense radiation and emergence of powerful jets. Shakura and Sunyaev [14] treated angular momentum transport in accretion disks as parameterized by an effective viscosity that was likely magnetic in origin. They described the stress using the so-called α viscosity prescription.

A critical breakthrough was when Balbus and Hawley [29, 30] found that weak magnetic fields are unstable to differential rotation and this can drive angular momentum radially outward, allowing gas to move radially inward. This instability leads to an effective viscosity by ultimately leading to turbulence and a self-sustaining dynamo. However, in disks with strong magnetic fields, suggested by Narayan et al. [39], the axisymmetric MRI is suppressed, meaning some new mechanism may be driving the angular momentum transport.

One possible source of stress leading to accretion onto compact objects is the effective viscosity generated by turbulence driven by the magnetic RT instability, as suggested in Elsner and Lamb [42, 43] and Arons and Lea [44, 45]. Since then, there have been many studies of this instability. Kaisig et al. [46], Lubow and Spruit [47], and Spruit et al. [48] examine the magnetic RT instability in a thin accretion disk with a vertical magnetic field. Li and Narayan [49] consider the interface between an infinitely thick accretion disk and magnetosphere around a central compact object,

generalized to be applicable to both neutron stars and BHs. Stone and Gardiner [62, 63] examine the magnetic RT instability in an astrophysical plasma with a variety of strong magnetic field configurations. Much work has also been studying the effect of this instability on neutron star accretion [64, 65, 66, 67, 68, 69, 70, 71]. It has also been seen in BH accretion disk systems [40, 41, 72, 73]. In these environments, the magnetic barrier is unstable and leads to null points in the magnetic field, allowing magnetic interchange between magnetic flux and mass. Once turbulence develops, a spectrum of modes develops. The large-scale modes correspond to a large portion of magnetic flux being ripped off the black hole. This magnetic flux pushes back into the disk, creating a low-density region, which we refer to as a bubble, in its wake. This process occurs many times during the thin (half-height H to radius R, $H/R \approx 0.1$) MADiHR simulation presented in Avara et al. [41]. Both the magnetic RT-driven turbulence and the large-scale magnetic flux seem likely drivers of angular momentum transport.

We study the magnetic-RT-driven turbulence and the large-scale magnetic interchange events and how these affect the effective viscosity and accretion rate of the disk. In Section 2.3, we describe the selection and visualization techniques developed as well as the stress calculations that were done. We discuss the results in Section 2.4, and provide conclusions in Section 2.5.

2.3 Methods

In this study, we use the MADiHR initially MAD thin disk ($H/R \approx 0.1$) simulation around a BH with dimensionless spin of $a/M = 0.5$, where a is the BH spin and M is the mass of the BH, presented in Avara et al. [41]. In the simulation, there are many times when the disk is disrupted by the magnetic flux coming off the BH due to the magnetic RT instability, the largest of these being the focus of this study.

To study the effects the magnetic RT instability has on the accretion rate of the disk, we need to know the mass accretion rate $\dot{M}$,

$$\dot{M} = \left| \int \rho u^r dA_{\theta\phi} \right|, \tag{2.1}$$

where ρ is the density, u^r is the radial 4-velocity, and $dA_{\theta\phi}$ is the differential surface area, and Υ_H, the strength of the dimensionless magnetic flux on the horizon,

$$\Upsilon_H(r) \approx 0.7 \frac{\int dA_{\theta\phi} 0.5 |B^r|}{\sqrt{\langle \dot{M}_H \rangle}} \Bigg|_{r=r_H}, \tag{2.2}$$

with horizon radius r_H, radial magnetic field strength B^r in Heaviside-Lorentz units and time averaged $\dot{M}$ on the horizon $\langle \dot{M}_H \rangle \approx 5.75$. Υ_H drops as large amounts of magnetic flux push into the disk as a result of the magnetic RT instability, shown in Fig. 2.1, so it can be used to define the lifespan of the RT bubble we studied, which is associated with the largest drop in Υ_H. We define the time period of interest by

finding the two maxima around this decrease in Υ_H, showing the bubble emerges at 31016 r_g/c and dissipates at 33240 r_g/c.

After identifying the period of interest, we study the RT bubble using both visualizations (Section 2.3.1) and calculations (Section 2.3.2).

2.3.1 Visualization

In this paper, we first perform a qualitative analysis of the magnetic RT instability. Detailed instability analyses are difficult (Li and Narayan [49]), and in the magnetic RT case are limited to very simple magnetic, density, and velocity profiles. Like Hirose et al. [74] and building on the density profiles of the equatorial plane of Igumenshchev [72], we sought to use 3D renderings to understand the structure of the magnetic field. We also generate a movie showing the evolution of the field. These renderings were made using vis5D+ [1]. Following prior work by McKinney et al. [40], to generate the frames, the coordinate basis quantities are converted to an orthonormal basis using the full metric in Kerr-Schild coordinates. This orthonormal basis is then converted to spherical polar coordinates and then Cartesian coordinates. We do not convert to Boyer-Lindquist time, and instead stick with Kerr-Schild time that is horizon-penetrating. The data is also interpolated from the original grid to a Cartesian grid. A resolution of 400^3 grid cells covers the inner region from -40 r_g to 40 r_g to focus on the disk very close to the black hole.

To track the magnetic field evolution through the lifetime of the RT bubble, we select certain magnetic field lines in the low density region and follow them through

[1]Freely available at: https://github.com/pseudotensor/Vis5dPlus .
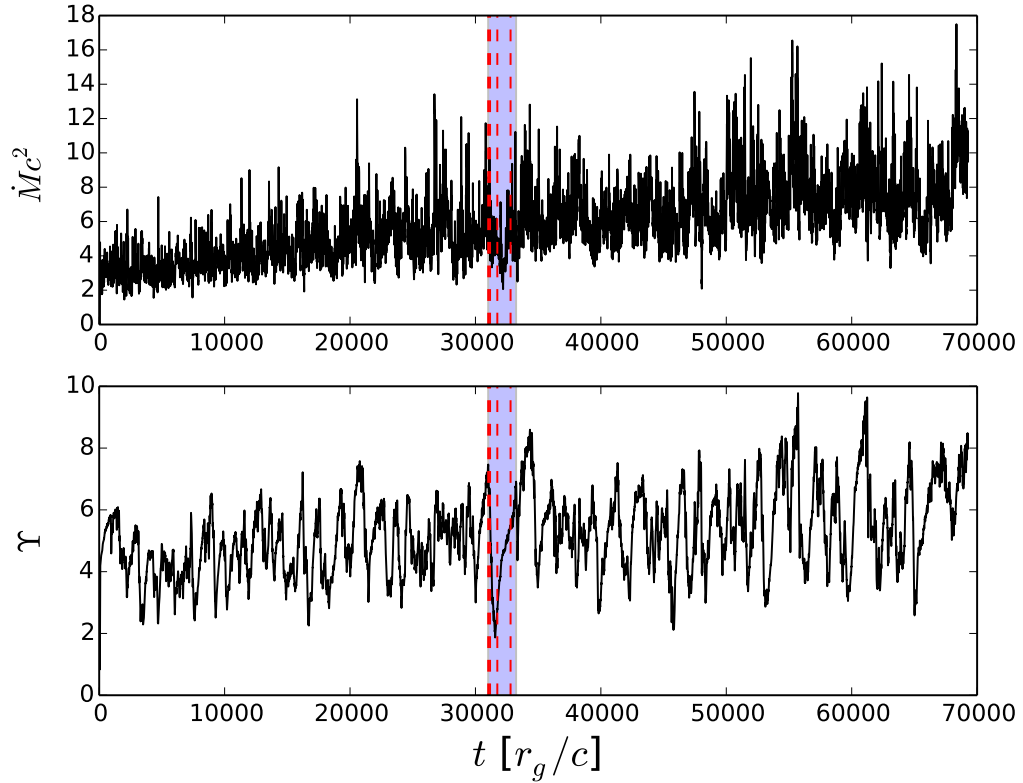
Figure 2.1: Quantities used to define the lifetime of the magnetic RT bubble. The upper panel shows the mass accretion rate through the BH, while the bottom panel shows the normalized magnetic flux threading it. The time period being studied is highlighted in blue with red dashed lines marking the times displayed in Fig. 2.2. The normalized flux provides a clearer picture of the dynamics around the BH, so it is used to determine the interesting time period. As magnetic Rayleigh-Taylor events occur, large amounts of magnetic flux move off the BH, but return to the BH as the bubble dissipates, so it is used to determine the lifespan of the RT bubble. For this project, we looked at the drop in magnetic flux that occurs between 31016 r_g/c and 33240r_g/c.

the time period of interest. We initially select field line seedpoints in the RT bubble

and disk midplane from the areas with high magnetic flux. This is done by creating

an unnormalized probability distribution for the midplane. The function used was

$$P\left(r,\phi\right) = \begin{cases} \left|\dfrac{B_z a_H}{\sqrt{\langle \dot{M}\rangle}\langle \Upsilon_H\rangle}\right|, & \text{for } r \leq r_H \\[2em] \left|\dfrac{\frac{r}{r_H}B_z a_H}{\sqrt{\langle \dot{M}\rangle}\langle \Upsilon_H\rangle}\right|, & \text{for } r > r_H \end{cases}, \tag{2.3}$$

with vertical magnetic field strength B_z, a_H is the surface area of the upper half

of the horizon, and time-averaged $\langle \Upsilon_H\rangle \approx 5.0$ as reported in Avara et al. [41]. We

developed this prescription based on Υ_H, with a dimensionless factor added to the

disk term to remove the radial dependence of the magnetic field. To normalize

this probability for use in selecting seedpoints, points with $P \leq 10$ were set to 0

and $P_{max}\left(t\right) = 5985.1$ is set to 1, and a linear function was created from those

fixed values. We chose to use the maximum single cell value of $P\left(t\right)$ rather than

an arbitrary cap to allow the probability function to most accurately represent the

high flux regions.

After the initial points are chosen, they are propagated forward in time using

the local fluid flow velocity. While this neglects magnetic diffusion processes, such as

reconnection, it does a reasonable job of keeping the field tied to the fluid flow. To

ensure the time-step used for each field line was small enough to accurately follow

its motion, the local Keplarian period is compared to the time between data files. If

the Keplarian period is much shorter than this time, an integer number of substeps

is used to interpolate between the data files, with the seedpoints' new locations

calculated using a velocity that is linearly interpolated between data files. After each step forward, the flux of the new position is checked using Equation 2.3. If the new probability is 0, meaning the point is now outside the RT bubble, we drop that point and a new one is randomly chosen to replace it.

To visually represent the amount of flux in the disk at a given time, we vary the number of seedpoints displayed. As the flux in the disk grows, the number of seedpoints $N(t)$ at a given time t ranged from $N_{min} = 15$ to $N_{max} = 30$ as

$$N(t) = max\left(N_{max}\frac{\sum P(t)}{(\sum P)_{max}}, N_{min}\right),$$ (2.4)

increasing as flux moved into the disk from the BH and decreasing as the flux was reprocessed by the disk. Finally, we fix a set of four field lines to $r = 0.75r_H$ initially evenly spaced in ϕ over the upper hemisphere of the horizon to show the evolution of the field in the jet region during this time. In Fig. 2.2, we show the field structure at four characteristic times: before the bubble forms, the emergence of the bubble from the BH, the peak of the bubble's size, and the dissipation of the bubble.

2.3.2 Stress Analysis

Because of the large vertical magnetic field that characterizes the MAD state, we want to consider not only the usual Maxwell stress,

$$\alpha_{r\phi} = -\frac{b^r b_\phi}{\langle P_b + P_{gas}\rangle},$$ (2.5)

(a) Quiescent

(b) Emergence

(c) Peak

(d) Dissipation
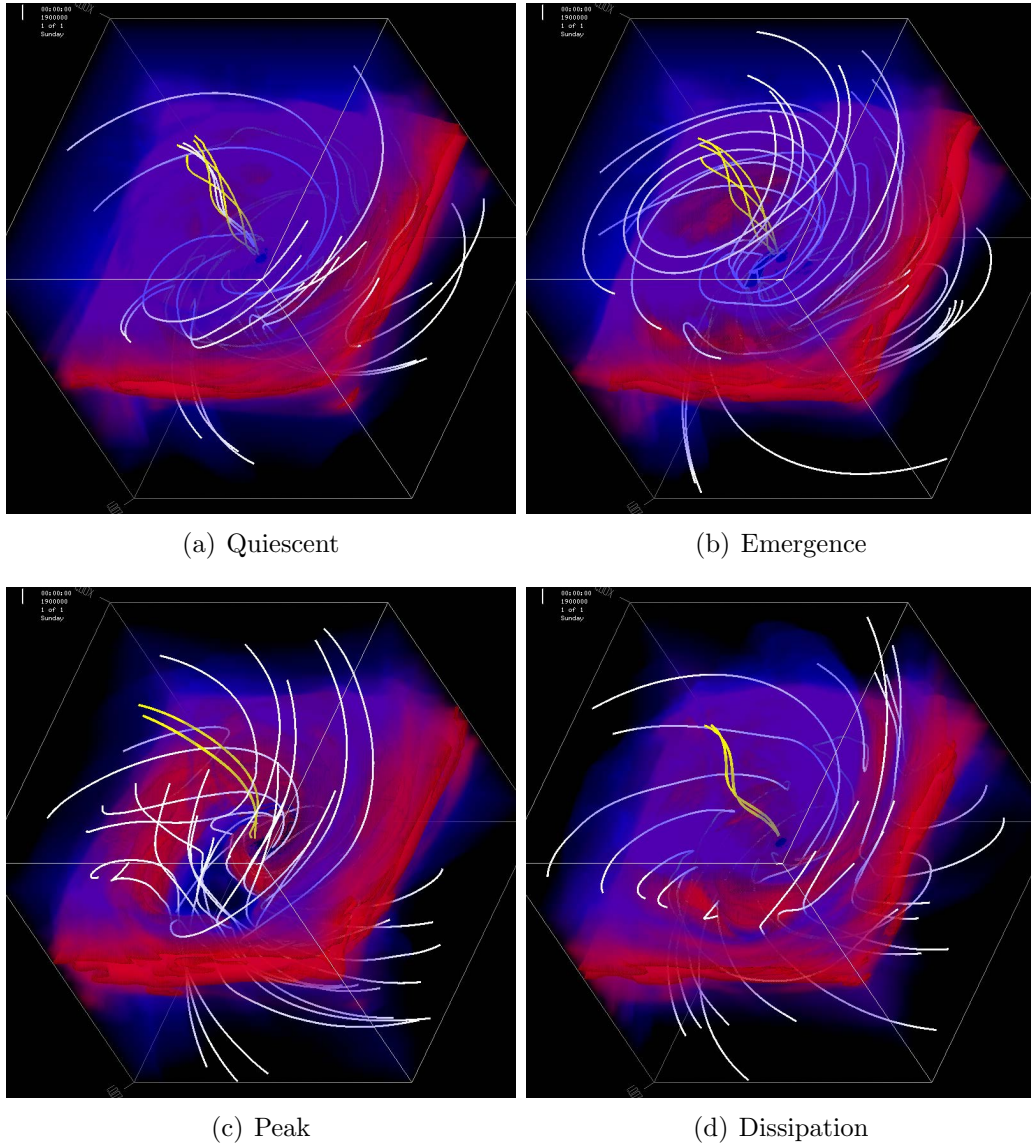
Figure 2.2: 3D renderings of key moments during the lifetime of the RT bubble in a cube $-40r_g \leq r \leq 40r_g$ on each side. Field lines chosen from the flux probability distribution are shown in white and the field lines fixed to the horizon are yellow. The disk is shown in red, while the corona is blue. From this, we see that as the RT bubble evolves, the magnetic field becomes less cohesive and more turbulent as in Fig. 2.2(c) , then returns to the previous orderly structure as the bubble dissipates (Fig. 2.2(d)). A video of the bubble's evolution can be found here: https://youtu.be/Sfh9O6Nm5Cc and a video of the seedpoints being followed in the midplane can be found here: https://youtu.be/74CuoWN2HjI

but also look at any vertical analog that might lead to angular momentum carried off in a wind,

$$\alpha_{z\phi} = -\frac{b^z b_\phi}{\langle P_b + P_{gas} \rangle},$$ (2.6)

where $P_b = b^\mu b_\mu/2$ is the magnetic pressure, $P_{gas} = (\Gamma - 1)u_g$ is the ideal gas pressure with adiabatic index $\Gamma = 4/3$. b^μ is the contravariant fluid-frame magnetic 4-field and is related to the laboratory-frame 3-field by $b^\mu = B^\nu h^\mu_\nu/u^t$, where $h^\mu_\nu = u^\mu u_\nu + \delta^\mu_\nu$ is a projection tensor and δ^μ_ν is the Kronecker delta function.

Though we know the axisymmetric MRI is suppressed in this simulation as reported in Avara et al. [41], the magnetic RT instability itself creates turbulence. Therefore, to separate the contributions to the angular momentum transport due to turbulence vs. the large vertical field, we decompose the magnetic field into a mean field term plus fluctuations ($b^\mu = \langle b^\mu \rangle + \delta b^\mu$). Then the (unnormalized) stress decomposition became

$$\alpha_{\mu\phi} = \langle b^\mu b_\phi \rangle + \langle b^\mu \rangle \delta b_\phi + \delta b^\mu \langle b_\phi \rangle + \delta b^\mu \delta b_\phi$$ (2.7)

The total radial and vertical stresses as well as the decomposed stress terms are calculated in both the disk and corona. These regions were defined only in terms of angular extent, with no density weighing or other such factors. The angle was chosen using half-height to radius $H/R \approx 0.1$ and the small angle approximation to give $\theta = 0.1$, so the disk is defined as $\frac{\pi}{2} \pm 0.1$ and the corona is $\frac{\pi}{2} \pm 0.1$ to $\frac{\pi}{2} \pm 0.2$. In Fig. 2.3, the total stress results are plotted from the start of the simulation until

after the bubble being studied dissipated (33240 r_g/c), while in Fig. 2.5, the stress decomposition is shown.

We also examine the differences between the stress in the RT bubble and in the high density area. The regions are separated using the plasma parameter $\beta = P_{gas}/P_b$ as a filter, with $\beta \leq 0.1$ considered the RT bubble region and higher values being the higher density region. The total stress in these areas is shown in Fig. 2.4 and the stress decomposition over the lifetime of the RT bubble is shown in Fig. 2.6.

2.4 Results and Discussion

2.4.1 Visualization

In the first snapshot Fig.2.2(a), we see the steady state of the disk. The field on the BH is helical and very tightly wound and the field in the disk has the same general shape, though looser in structure. Moving forward in time to the emergence of the bubble (Fig. 2.2(b)), the magnetic field in these regions begin to unwind and become less ordered. This is even more prominent in the snapshot of the bubble at its maximal size, Fig. 2.2(c). Here the field is much more tangled, having been swept back by the slower rotation of the bubble in the disk. Also, the field in the jet region is almost vertical, with much less winding. Finally, as the bubble begins to dissipate in Fig. 2.2(d), the field becomes ordered again with the field in the jet region twisting up once more, which is also discussed in Igumenshchev [72].
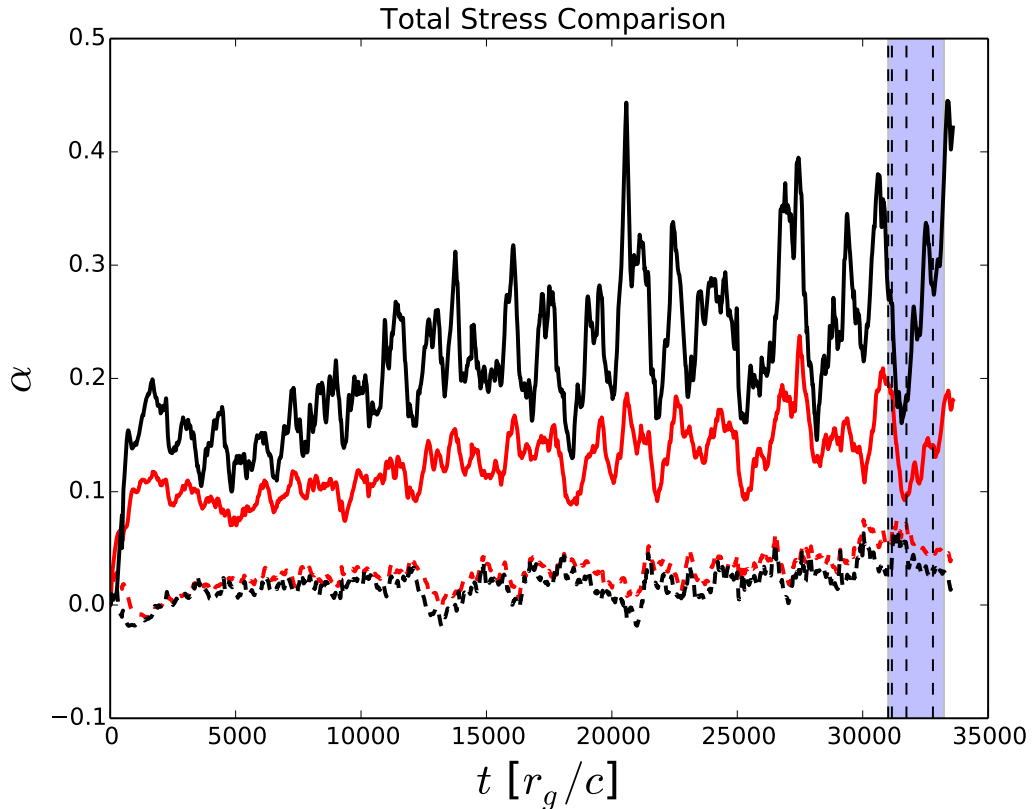
Figure 2.3: Long term stress in the disk (black) and corona (red). The vertical stress is shown as a dashed line, while the radial stress is solid. The time period being studied is highlighted in blue with vertical dashed lines marking the times displayed in Fig. 2.2. As the bubble emerges, the radial stress in both regions decreases, but grows as the bubble dissipates, indicating that stress, and therefore accretion, increase after the lifetime of the bubble; however, the vertical stress increases slightly while the bubble is moving through the disk.

2.4.2 Stress Analysis

In Fig. 2.3, we plot the total radial stress integrated over all ϕ, $10r_g \leq r \leq 40r_g$, and the θ ranges given above for the disk and corona are shown. The vertical stress is integrated over the same ϕ and radial regions, but the upper and lower halves of the θ region are calculated separately, then subtracted from each other to ensure that positive stress corresponds to outgoing angular momentum transport. The
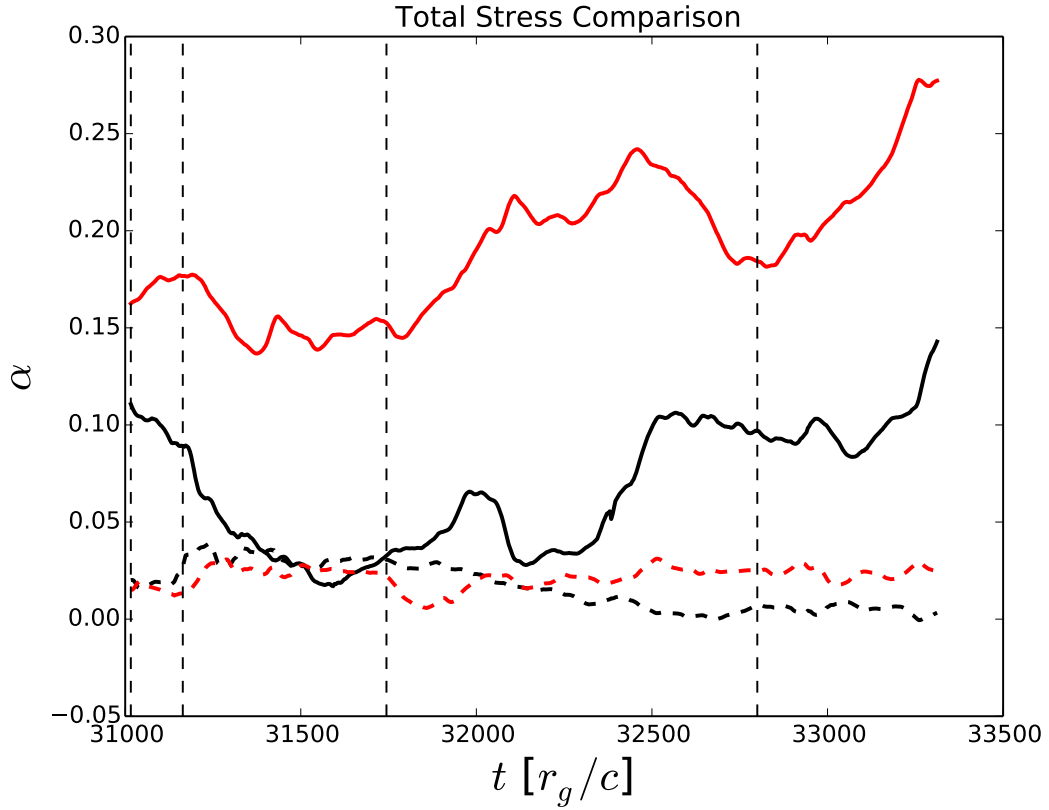
Figure 2.4: Division of stress in the RT bubble (black) and the higher density portion (red) of the disk for the lifetime of the RT bubble. The radial stress is shown as a solid line, while the vertical stress is a dashed line. The vertical dashed lines mark the times displayed in Fig. 2.2. As the bubble expands, the radial stress in the bubble decreases, while the vertical stress increases. Outside the bubble, both the radial and vertical stress start to increase as the bubble dissipates around 32000 r_g/c, with the radial stress almost doubling by the time the bubble disappears.

radial stress through the disk is the dominant term, much higher than the vertical stress even with the large vertical field that characterizes the MAD state. In the corona, radial stress is also higher than the vertical term. However, the vertical stress in the corona is slightly higher than in the disk, indicating the vertical outflows are more prominent there. The radial stress is always positive, corresponding to outward angular momentum transport and enhanced accretion, while the vertical stress is negative at some times, but is usually positive.

(a) Radial Disk

(b) Radial Corona

(c) Vertical Disk

(d) Vertical Corona
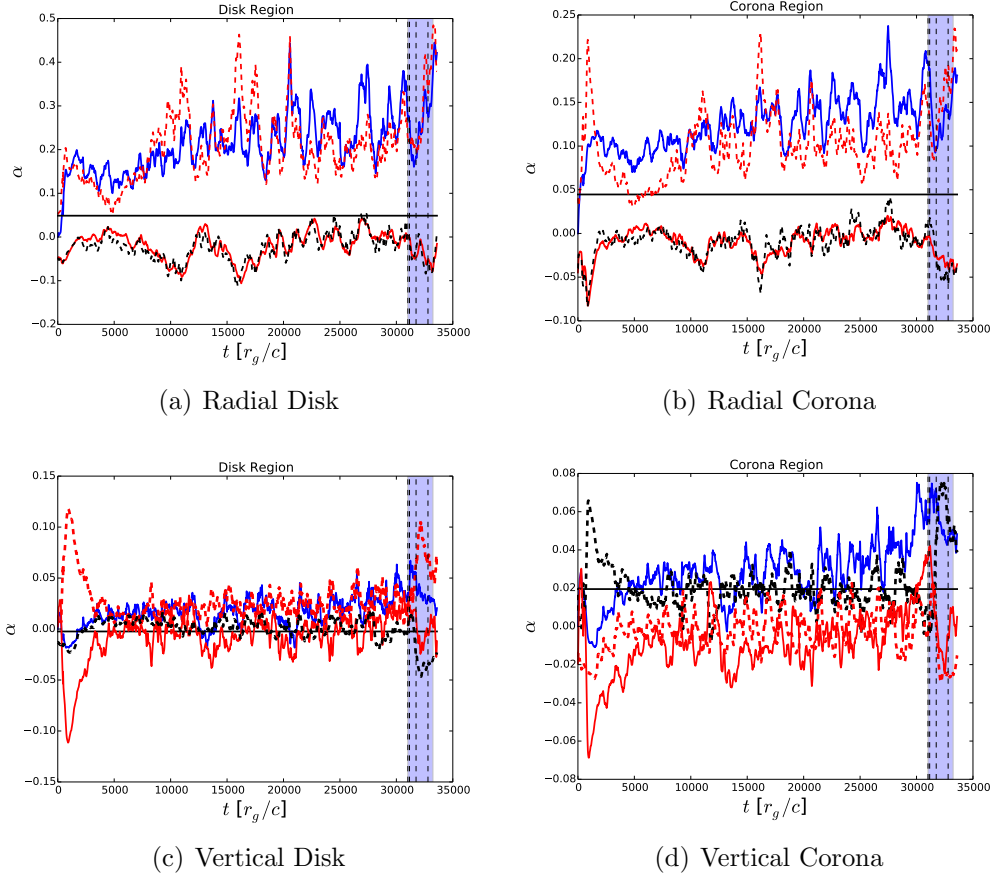
Figure 2.5: The decomposition of the total stress (blue solid line) into mean field (black solid), purely turbulent (red dashed), and 2 mixed terms ($\langle b^i \rangle \delta b_\phi$ as a red solid lines and $\delta b^i \langle b_\phi \rangle$ as a black dashed line). The time period being studied is highlighted in blue with vertical dashed lines marking the times displayed in Fig. 2.2. The upper panels show the radial stress decomposition in the disk (left) and corona (right) while the lower panels are the vertical stress in the disk (left) and corona (right). In both regions, the radial stress is dominated by purely turbulent component, despite the suppression of the MRI. As for the vertical stress, in the disk, the stress components fluctuate around 0, but seem to be net positive. In the corona, the turbulent terms are negative, but the mean field term is positive, meaning it contributes to outward angular momentum transport.

(a) Radial stress in the RT bubble

(b) Radial stress outside the RT bubble

(c) Vertical stress in the RT bubble

(d) Vertical stress outside the RT bubble
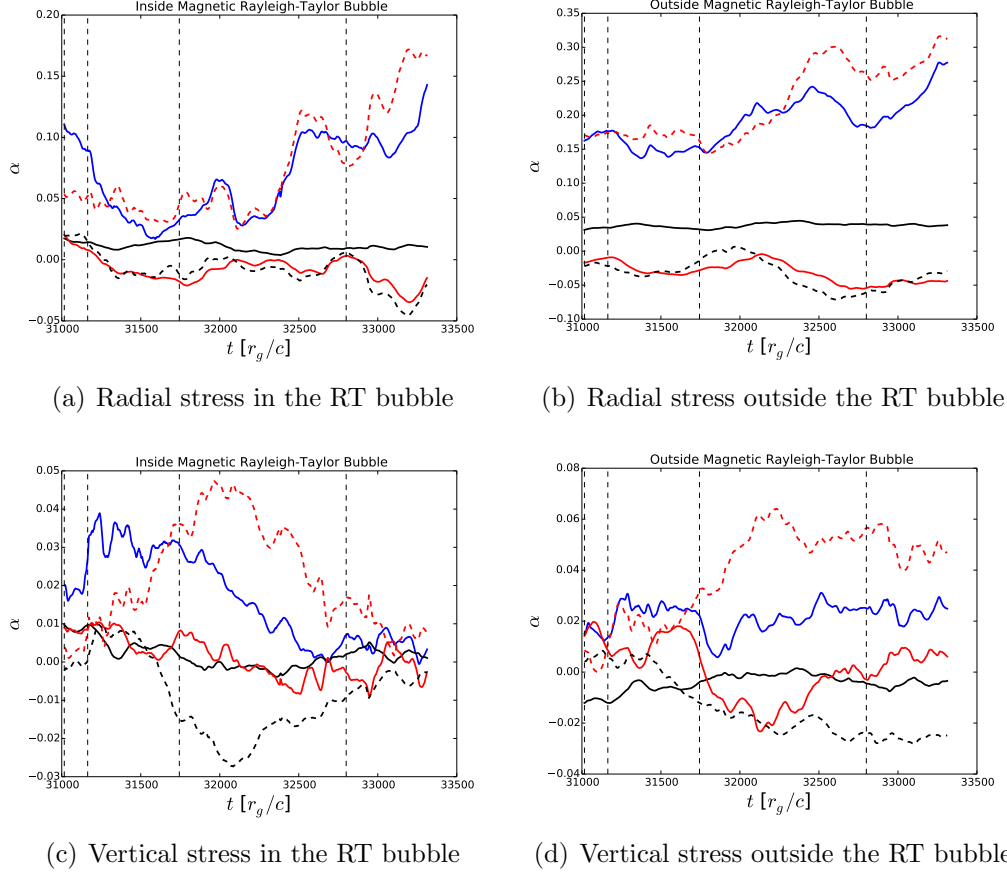
Figure 2.6: The decomposition of the total stress (blue solid line) into mean field (black solid), purely turbulent (red dashed), and 2 mixed terms ($\langle b^i \rangle \delta b_\phi$ as a red solid lines and $\delta b^i \langle b_\phi \rangle$ as a black dashed line). Vertical dashed lines mark the times displayed in Fig. 2.2. The upper panels show the radial stress decomposition inside (left) and outside (right) the RT bubble while the lower panels are the vertical stress inside (left) and outside (right) the RT bubble. The total vertical stress is close to 0 for the lifetime of the bubble and we see that the component terms mostly balance themselves out. In both regions, the total radial stress is dominated by the purely turbulent term and positive, leading to angular momentum transport.

Looking more closely at the terms of the stress decomposition in Fig. 2.5, integrated over the same volume as Fig. 2.3, we see that the leading component of the radial stress is the purely turbulent term, even though the MRI is suppressed. This turbulence can easily be driven by the magnetic RT-instability instead of the MRI. This agrees with Fig. 2.2(c), which shows the magnetic field structure becoming less ordered and more turbulent as the RT bubble reaches its maximum extent. The mean field term also contributes positive stress, therefore outward angular momentum transport, in both the disk and corona with roughly the same strength. The mixed radial stress terms are the smallest components and mostly negative, meaning inward angular momentum transport opposing accretion. In the vertical case, the mean field and the purely turbulent components are roughly equal in magnitude in both regions. In the disk, all terms of the decomposition fluctuate around the mean field term at 0. Other than the $\langle b^z \rangle \delta b_\phi$ at early times, most of these fluctuations are positive, so angular momentum is transported out of the system except at for these early times. In the corona, though the purely turbulent or mixed terms fluctuate into negative values often, the mean field term is positive, meaning that the ordered field in the corona is prominent in the accretion process.

At the time the magnetic bubble emerges off the BH, the radial stress decreases while the vertical increases. Overall, this means the stress in the disk is lowered by the emergence of the bubble, hindering accretion. Looking at Fig. 2.4, the RT bubble contributes much less radial stress, up to a factor of four less at times. For the total vertical stress, though, the bubble actually has a higher contribution until it starts to dissipate. Once again, the turbulent component is the dominant

contribution to the stress, as seen in Fig. 2.6. The mixed terms again become negative in both parts of the disk. Interestingly, in Fig. 2.6(c), the mean field term is actually negative until the bubble begins to dissipate and the vertical flux is reprocessed into the disk. As the bubble dissipates, the stress begins to rise again in both parts of the disk and a spike can be seen in Fig. 2.3 after it is reabsorbed by the disk. The strength of the turbulent stress indicates that a secondary instability is creating a turbulent field in the wake of the RT bubble.

2.5 Conclusions

We studied how the magnetic RT instability affects the evolution and angular momentum transport in thin accretion disks in the MAD state by investigating the largest of many RT bubbles produced in the MADiHR simulation from Avara et al. [41]. We started by developing the first 3D visualization technique to select and follow magnetic field lines in the high flux regions of the bubble. This showed us how the emergence of the RT bubble leads to less ordered magnetic field in the disk and less twisted up field in the jet region, indicating that the magnetic RT instability is leading to a secondary turbulence in the disk. This visualization method is applicable to many other situations where the magnetic field is disrupted, such as magnetic field inversions or magnetic plasma instabilities in other disk geometries.

We also examined the effects of the RT bubble through stress calculations. We found the dominant contribution to the stress in both the disk and corona is the radial term with the vertical stress up to four times smaller than the radial term.

We also saw that the emergence of the RT bubble corresponds to a reduction in radial stress in both the disk and corona, but an increase in the vertical stress.

When the stress terms are decomposed into mean field, purely turbulent, and mixed components, we measure the turbulent component to be dominant, despite the suppression of the MRI. Only in the vertical stress is the mean field contribution as strong as the turbulent one. As seen in the visualization, this turbulence is linked to the emergence of the bubble, so could be due to a secondary instability caused by the magnetic RT instability.

In the bubble itself, the stress is suppressed much more than in the higher density region. Though the vertical stress is much smaller than the radial stress, it is stronger in the bubble than the disk until the bubble starts to dissipate. As seen in the disk, the turbulent field is the dominant driver of the stress, while the mean field term is a factor of 3-4 smaller. Again, this is consistent with the disordered field lines seen in the visualization.

These results are limited by the simplified treatment of the thermodynamics of the accretion disk. To keep the disk close to the target scale height of $H/R \approx 0.1$, an ad hoc cooling function was employed, rather than a more complete handling of the thermodynamics. While this might have kept the disk thinner than a more complex cooling function, we see similar low-density regions created by the magnetic RT instability in simulations of thicker disks, so our results would still hold if the disk in this work were thicker.

The extra dissipation produced by the thin MAD state could lead to more emission from near and within the inner-most stable circular orbit (ISCO). In prior

studies of the emission, the corrections to the spin predictions are minimal except at low spin [75] with higher-energy emission from near the ISCO. Indeed, the emission is marginally optically thin and could be dominated by non-thermal emission. Our results suggest that, despite the magnetic field having a large-scale ordered component in the MAD state, the disk is still dominated by turbulent viscosity driven by magnetic RT instabilities and the MRI. The magnetic RT instabilities form even within the ISCO due to the magnetic field piling-up against the BH, and so they could be an important source of extra emission from within the ISCO.

We hope our visualization and basic analysis of the stress in the accretion disk will drive more analytical and simulation work to understand the origin of angular momentum transport in MADs. We cannot conclude that the MRI is unimportant in MADs, but the magnetic RT plays an important role in controlling the effective viscosity by developing vigorous turbulence throughout the flow. While existing analytical analysis of magnetic boundaries in disks cannot be easily applied to these simulations, we plan to next study the magnetic stability directly within the simulation by tracking passive mode growth as done in Guan and Gammie [76]. By injecting modes, we can directly trace their evolution to see if they behave as expected from the MRI instability or as from the magnetic RT instability.

Acknowledgements

Chapter 3: Observational Signatures of the Magnetic Rayleigh-Taylor Instability in Thin MADs

3.1 Abstract

The inner workings of accreting supermassive black hole (SMBH) systems have been studied for many years, but these studies have been restricted to simulations as observational capabilities have been insufficient to probe the details of the complicated plasma and magnetic field interactions occurring in these systems. Since the Event Horizon Telescope (EHT) has published images of the innermost regions of the M87 system, we are now in an era where it is possible to look into the heart of a SMBH accretion disk and detect the signature of the plasma physics occurring there. To understand what might soon be seen, we have conducted an exploratory study of the observational signatures of the magnetic Rayleigh-Taylor instability, which occurs frequently in magnetically arrested disk (MAD) simulations. Our preliminary analysis shows a very strong similarity between the dimensionless magnetic flux on the black hole (BH) horizon Υ_H and the simulated light curves. We also see visibility nulls in intensity images associated with the low density bubble created by the magnetic Rayleigh-Taylor (RT) instability.

3.2 Introduction

AGN have been of great interest to astronomers for many years; however, many of their features remain unexplained due to the limitations of observational capabilities. Until very recently, the innermost regions, where many exotic phenomena originate, were unobserved and could only be studied in detail via three-dimensional (3D) general relativistic magnetohydrodynamic (GRMHD) simulations. Now the Event Horizon Telescope (EHT) has the ability to probe these regions because of the high observing frequency (230 GHz), resolution, and sensitivity. Most notably, in April 2019, the EHT collaboration published the first event-horizon-scale images of M87 [77, 78, 79, 80, 81, 82], opening a new realm of possibilities in studying AGNs. As a bridge between the detailed simulations and potential observations, radiative transfer calculations can be performed to simulate spectra and snapshots. Many of these studies have been done in preparation for the EHT observations by members of the collaboration. Many features of M87 and Sgr A* have been investigated using radiative transfer techniques to simulate EHT results, including jets [83, 84, 85], magnetic field structure [86], and the geometry of the innermost regions near the BH [87, 88].

One question in particular that can be studied this way is AGN variability, which has been a focus of research for many years and is one of the characteristics that separates AGN from other systems, but a definite cause is not yet known [4, 5]. This variable emission is seen at many wavelengths, over many timescales, and is common across many different systems, from supermassive black holes (SMBH) to

solar mass BHs in X-ray binaries, suggesting the existence of a shared physical process creating it, likely an accretion process [5, 89, 90]. This could be mediated by the magnetic field structure near the BH [91]. Park and Vishniac [92] suggest that radial transport of polodial field is linked to variability and changes in the magnetic field strength are correlated to variability in a study by Goldston et al. [93]. Dexter and Begelman [94] discuss how the standard disk theory doesn't fully explain observations of variable AGN luminosity, but disks supported by large magnetic fields may offer a better model. Zamaninasab et al. also showed that a disk model with a higher magnetic field strength, specifically a model that is in the magnetically arrested disk (MAD) state characterized by large polodial magnetic fields, is an accurate model for radio-loud AGN [35, 95]. The tight correlation they found between accretion disk luminosity and magnetic flux in the jet, which is related to the flux on the BH horizon Υ_H, reveals an interesting possibility for the source of AGN variability. In the very thin MAD model presented in Avara et al. [41], the accretion disk is dramatically affected by these fluctuations, offering an ideal model to use for the exploration of the link between the magnetic flux and AGN variability. Using Sgr A* as our physical model, we simulate spectra to probe this possible link. Previous studies of the variability of Sgr A* have been done using radiative transfer techniques (e.g. Chan et al. [96] and Medeiros et al. [97]), but these have focused on the impact of the accretion flow directly rather than the relationship between the magnetic field structure and variability.

We are also interested in discovering any possible observational signatures the magnetic RT instability might create. Magnetic RT effects have been observed

in laboratory plasmas [98, 99], solar prominences (for review, see Hillier [100]), further out into interplanetary space [101], and supernovae and their remnants [102]. However, while this instability has been seen in simulations of SMBH systems (e.g. McKinney et al. [40], Avara et al. [41], Marshall et al. [1]), as well as neutron stars (e.g. Romanova et al. [68], Kulkarni and Romanova [69], Blinova et al. [71]), it has not be observed in these environments, so we have also created synthetic intensity images for the largest magnetic RT event that occurs in the simulation to look for possible observational signatures that could be seen by the EHT, extending the work done in Chapter 2.

This paper is organized as follows. In Section 3.3, we describe the methods and model used in this work, including the radiative transfer scheme used to generate the simulated observations. In Section 3.4, we describe and discuss our preliminary results, and in Section 3.5, we summarize our findings.

3.3   Method

In this section, we describe the GRMHD simulation that was studied, the general relativistic polarized radiative transfer technique used, and the parameters used to generate the simulated data sets.

3.3.1   GRMHD Simulation

For this work, we use a previously published GRMHD simulation created with the code HARM [28, 40], which solves the ideal MHD equations of motion in a Kerr

metric [16, 17]. This model is the MADiHR simulation from Avara et al. [41], which simulates a thin disk ($H/R \approx 0.1$) around a moderately spinning BH ($a/M = 0.5$) that is initialized with enough magnetic flux to be close to the magnetically-arrested disk (MAD regime), which it reaches by $\sim 5000 r_g/c$. Because this simulation was performed using a code without an internal radiative transfer scheme, an ad hoc cooling function was used to keep the disk thin and radiatively efficient.

Due to the strong vertical magnetic fields (plasma beta $\beta = P_{gas}/P_b = 50$, where P_{gas} is the gas pressure and P_b is the magnetic pressure), the axisymmetric magnetorotational instability (MRI) is suppressed, but there are many events where the disk is disrupted by a low density bubble created by the magnetic RT instability. Because of the thinness of the disk, these events have a dramatic effect on the simulation, the largest of which was studied in the previous chapter (see also [1]). Here we present simulated observations associated with that event.

3.3.2 Electron Temperature Prescription

While HARM does not directly compute the temperature of either electrons or protons, it is necessary to know these quantities in order to calculate the emission from the disk. We follow Shcherbakov et al. [51] in our treatment of them, which is based on collisionless physics described in Sharma et al. [103]. The simulation data are extended via power law extension to the Bondi radius of Sgr A*, $r_{out} = 3 \times 10^5 r_g$. Here the electron and proton temperatures are set to $T_e = T_p = 1.5 \times 10^7 K$ and are then evolved inwardly as a function of u_{gas}/ρ, the internal energy per unit rest mass,

considering the rate of proton-electron collisions. Beyond $r = 10^4 r_g$, collisions are frequent, keeping $T_e \approx T_p$, but as the radius decreases, the timescale for collisions increases, and T_e deviates from T_p as the electrons become relativistic. The electron-proton heating ratio is also important for determining the temperatures, as Sharma et al. [103] found

$$\frac{f_e}{f_p} = C_{heat} \sqrt{\frac{T_e}{T_p}}, \tag{3.1}$$

where $C_{heat} \sim 0.3$.

3.3.3   General Relativistic Polarized Radiative Transfer

To produce the simulated data, we used ASTRORAY [50, 51], a GR polarized radiative transfer code that uses data files from GRMHD simulations as inputs. This code computes the polarized synchrotron emission, absorption, Faraday rotation and conversion, using a thermal, isotropic electron distribution.

A uniform grid of geodesics are traced from an observer's image plane to the SMBH. Along these rays, the polarized fluxes are computed by integrating the intensities back to the image plane. To account for the changes in the simulation as the light propagates from the BH to the observer at time t_0, we include snapshots between $t_0 - \Delta t$ and $t_0 + \Delta t$. The value of Δt is chosen to be large enough to calculate accurate spectrum, but small enough that the calculations are not overly time-consuming.

This procedure outputs the Stokes parameters (I, Q, U, V). Here I is the intensity, V is the circular polarization, with $V > 0$ corresponding to right circu-

lar polarization following the IAU/IEEE convention. Linear polarization is $LP = \sqrt{|Q|^2 + |U|^2}$ and the linear polarization direction, known as the electric vector position angle (EVPA), is found using $EVPA = arg(Q + iU)/2$, measured EAST of NORTH. Polarization fractions are normalized by the intensity I and given in percent.

3.3.4 Model Fitting

The free parameters in this model are

1. inclination i,

2. accretion rate normalization $\dot{M}$,

3. heating constant C_{heat}, and

4. time span before and after a given time t_0 to account for the evolution of the simulation, Δt.

We chose three inclinations for this study: edge-on (90°), tilted (150°), and nearly face-on (170°). This allowed us to explore the range of possible inclinations, generalizing the results of this work. The accretion rate was determined by fitting our simulated flux to the mean value of $F_\nu = 2.64 \pm 0.14$ for $\nu = 230$GHz reported in Shcherbakov et al. [51]. In the present work, we only consider the $\nu = 230$GHz data, focusing on the EHT's current observational capabilities. We use the value of $C_{heat} = 0.3712$ from Shcherbakov et al. [51]'s best fit model for spin $a/M = 0.5$. Finally, we set $\Delta t = 240 r_g/c$.

We studied the inner regions ($|r| \leq 15r_g$) of the simulation during five time periods in the simulation, each between $2200r_g/c$ (12.8 hours for Sgr A*) and 2400 r_g/c (14 hours for Sgr A*), sampling the data every $4r_g/c$ (1.4 minutes for Sgr A*), examining the magnetic RT bubble from Marshall et al. [1] ($31016 - 33232r_g/c$) as well as four quiescent periods of similar length (32000-34400 r_g/c, 35800-38000 r_g/c, 53600-56000 r_g/c, and 67000-69268 r_g/c). The calm periods were chosen for the low fluctuations in Υ_H, the dimensionless magnetic flux threading the BH horizon, which is given by

$$\Upsilon_H(r) \approx 0.7 \frac{\int dA_{\theta\phi} 0.5|B^r|}{\sqrt{\langle \dot{M}_H \rangle}} \Bigg|_{r=r_H}, \tag{3.2}$$

with horizon radius r_H, radial magnetic field strength B^r in Heaviside-Lorentz units and time averaged $\dot{M}$ on the horizon $\langle \dot{M}_H \rangle \approx 5.75$ (Fig. 3.1). This is coupled with a lack of large low density bubbles in the video of the disk's evolution within the region we are studying (found here: https://youtu.be/t1vaW3ByM8Y). For each of these time periods, images of the average intensity were plotted, as well as light curves over the whole simulation for each inclination. Additionally, images of particular snapshots for the four times highlighted in Chapter 2 (31016 r_g/c, 31164r_g/c, 31744r_g/c, and 32816r_g/c) were created and compared to the 3D renderings shown in Fig. 2.2.
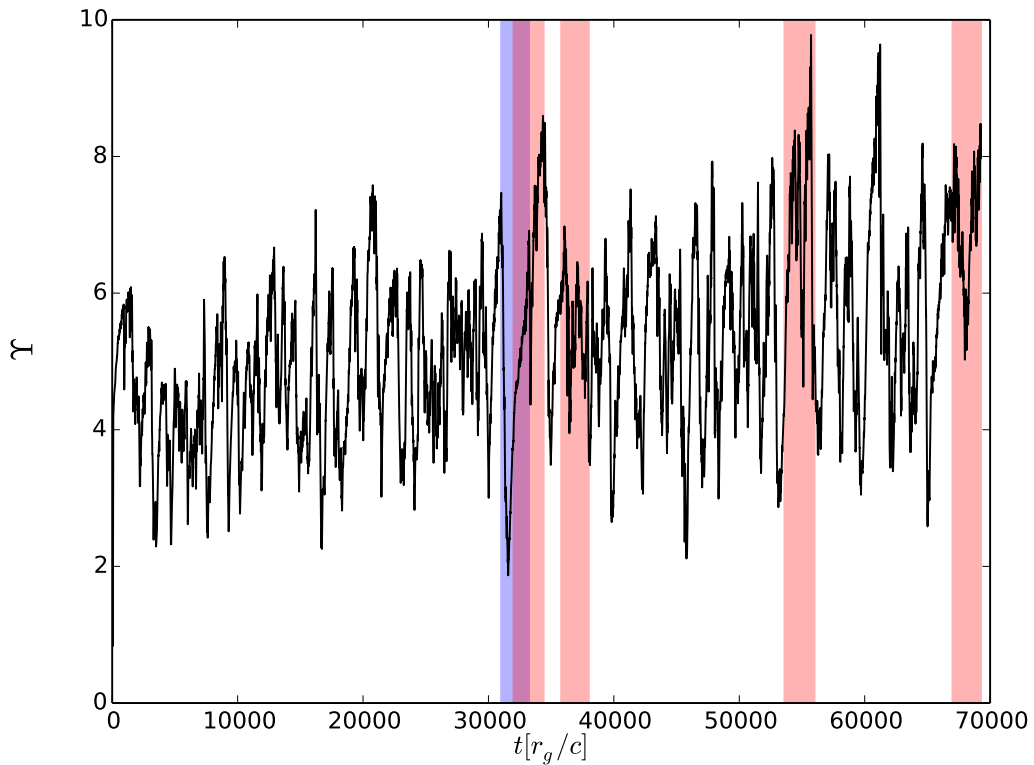
Figure 3.1: Normalized magnetic flux threading the BH vs time, with the shaded regions indicating the time periods studied in this paper. The blue period is the magnetic RT event studied in Marshall et al. [1] from $31016-33232r_g/c$, while the red regions are the quiescent times (32000-34400 r_g/c, 35800-38000 r_g/c, 53600-56000 r_g/c, and 67000-69268 r_g/c).
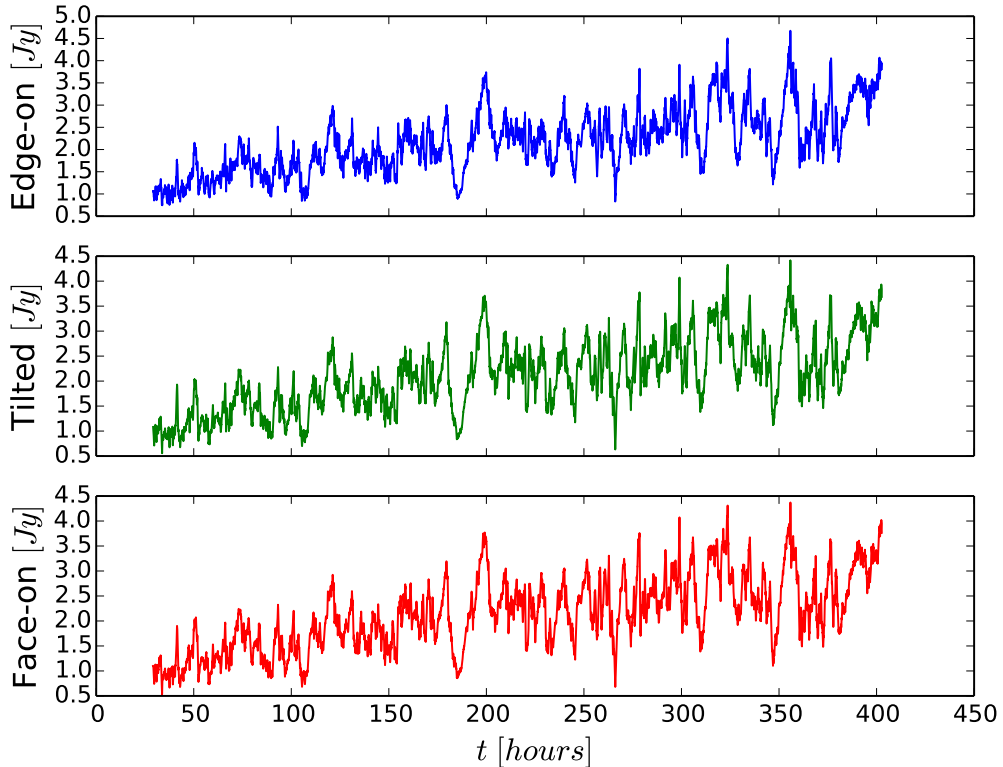
Figure 3.2: Simulated light curves for each of the inclinations (top: edge-on, middle: tilted, bottom: face-on) studied in this work, from $t = 5000r_g/c \approx 30$ hours when the disk reaches the MAD state until $t = 69028r_g/c \approx 400$ hours. While they are very similar in shape and amplitude, the edge-on case has both a higher average and maximum intensity.

3.4   Results and Discussion

3.4.1   Simulated Light Curves

First we present the simulated light curves for the 230 GHz flux in Fig 3.2 at each of the three inclinations considered. We ignore the times before our model reaches the MAD state ($t = 5000r_g/c \approx 30$ hours) and $\Delta t = 240r_g/c = 1.4$ hours from the end of the simulation.

We see that while the inclination angle slightly changes the amplitude of the

47
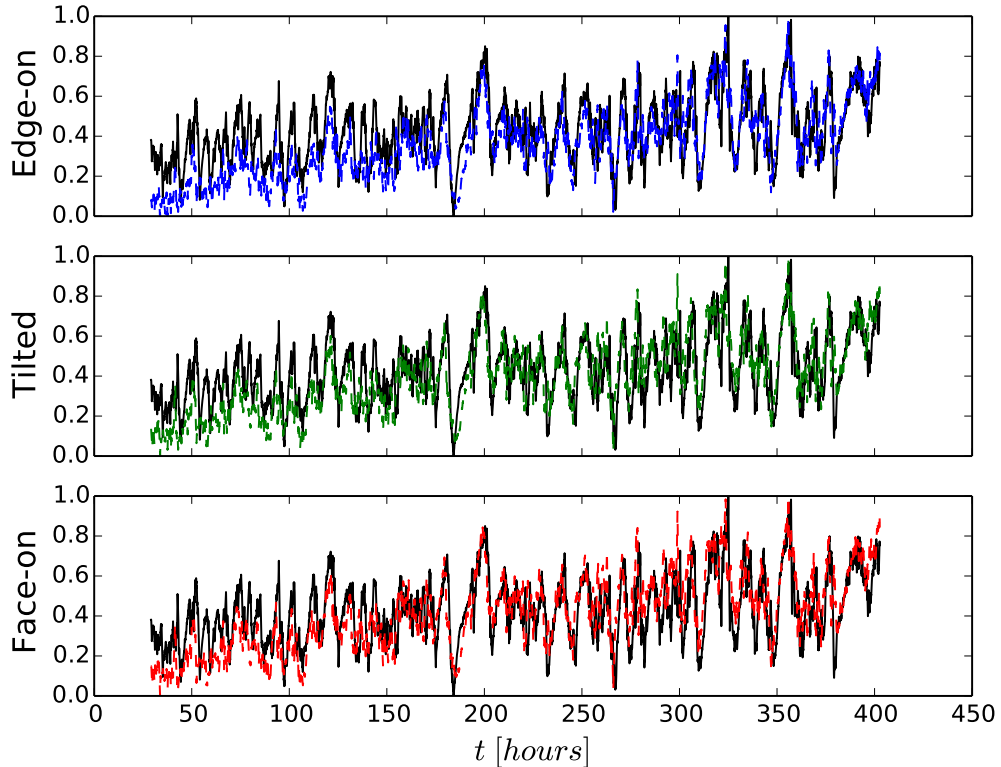
Figure 3.3: Normalized Υ_H (black) and I (color) versus time for each of the inclinations (top: edge-on, middle: tilted, bottom: face-on) from $t = 5000 r_g/c \approx 30$ hours when the disk reaches the MAD state until $t = 69028 r_g/c \approx 400$ hours. Here we see that the two quantities are remarkably similar in structure, especially after $t = 30000 r_g/c$ or 175 hours.

curve, the overall shape is consistent. This indicates that the flux is more strongly influenced by the underlying physics and intrinsic properties of the system rather than extrinsic ones such as viewing angle. The edge-on orientation has a marginally higher intensity than the other inclinations and the face-on inclination has a higher intensity than the tilted one.

These light curves also appear to share the main features of the Υ_H vs t plot shown in Fig. 3.1. To explore these similarities, we vertically shifted and normalized these quantities so that they ranged from 0 to 1 in amplitude then plotted them next
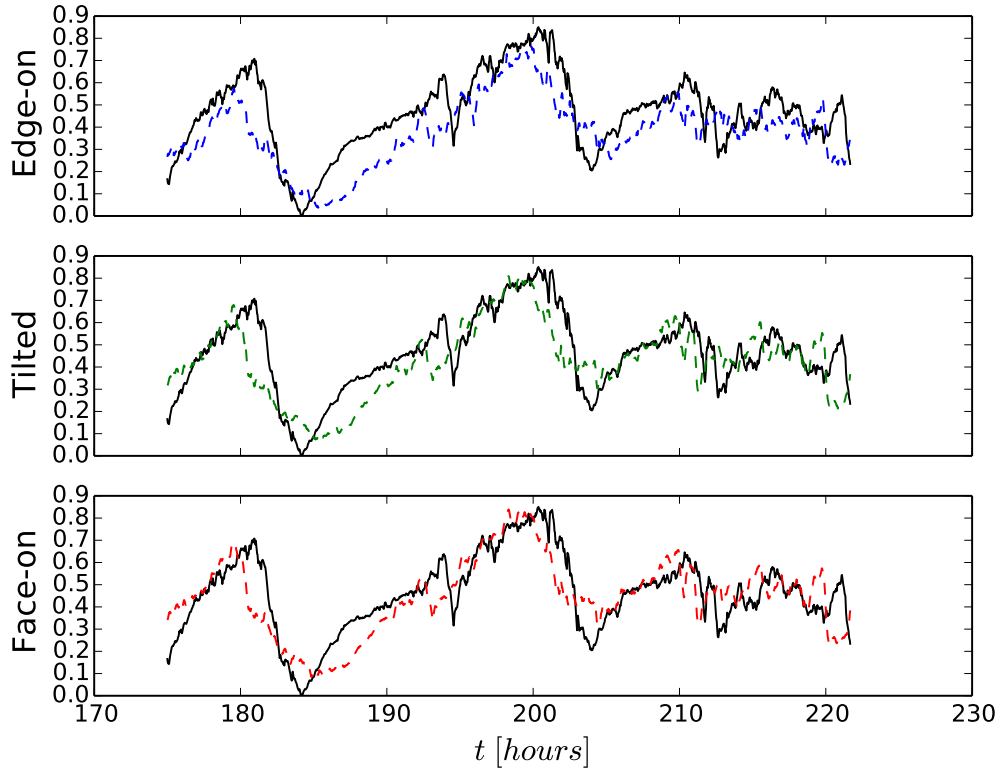
Figure 3.4: Normalized Υ_H (black) and I (color) versus time for each of the incli-
nations (top: edge-on, middle: tilted, bottom: face-on) from $t = 30000r_g/c = 175$
hours to $t = 38000r_g/c \approx 222$ hours. This window includes the magnetic RT event
and the first two quiescent periods and shows that I tends to decrease before Υ_H,
but rises after, broadening the shared features.

to each other for easier comparison, shown in Fig. 3.3. This shows the magnetic flux on the horizon and the radio luminosity to be even more strikingly similar, particularly after $t = 30000r_g/c$ (175 hours). Only during the magnetic RT event studied in Chapter 2, after the low density bubble reaches its maximal size, is there a large variance between the curves. Neither quantity seems to be leading or lagging behind the other for the whole period shown, but alternating which signal leads the other, as I tends to decrease earlier than Υ_H and vice versa, as seen in Fig. 3.4.

3.4.2   Average Intensity Images

Here we present the simulated averaged intensity images for the periods identified above. The images presented here are not adjusted to simulate the effects of scattering as the radiation passes through the interstellar medium. This will be accounted for in future work.

Fig. 3.5 shows the average intensity image for the edge-on orientation, Fig. 3.6 shows the tilted orientation, and Fig. 3.7 the nearly face-on orientation. Again, the edge-on case has a higher intensity than the others, despite little emission coming from the narrow band of the disk across the center of the image.

In each case, the same features are seen. The image is dimmest during the period of time over the magnetic RT event (Figs. 3.5(a), 3.6(a), and 3.7(a)), due to the much lower density of the region while the magnetic RT bubble is moving through it. This period will be considered in more detail in Sec. 3.4.3.

For the other times considered, the image brightens as the magnetic flux is

(a) $t = 31016 - 33232 r_g/c$

(b) $t = 32000 - 34400 r_g/c$

(c) $t = 35800 - 38000 r_g/c$

(d) $t = 53600 - 56000 r_g/c$

(e) $t = 67000 - 69268 r_g/c$
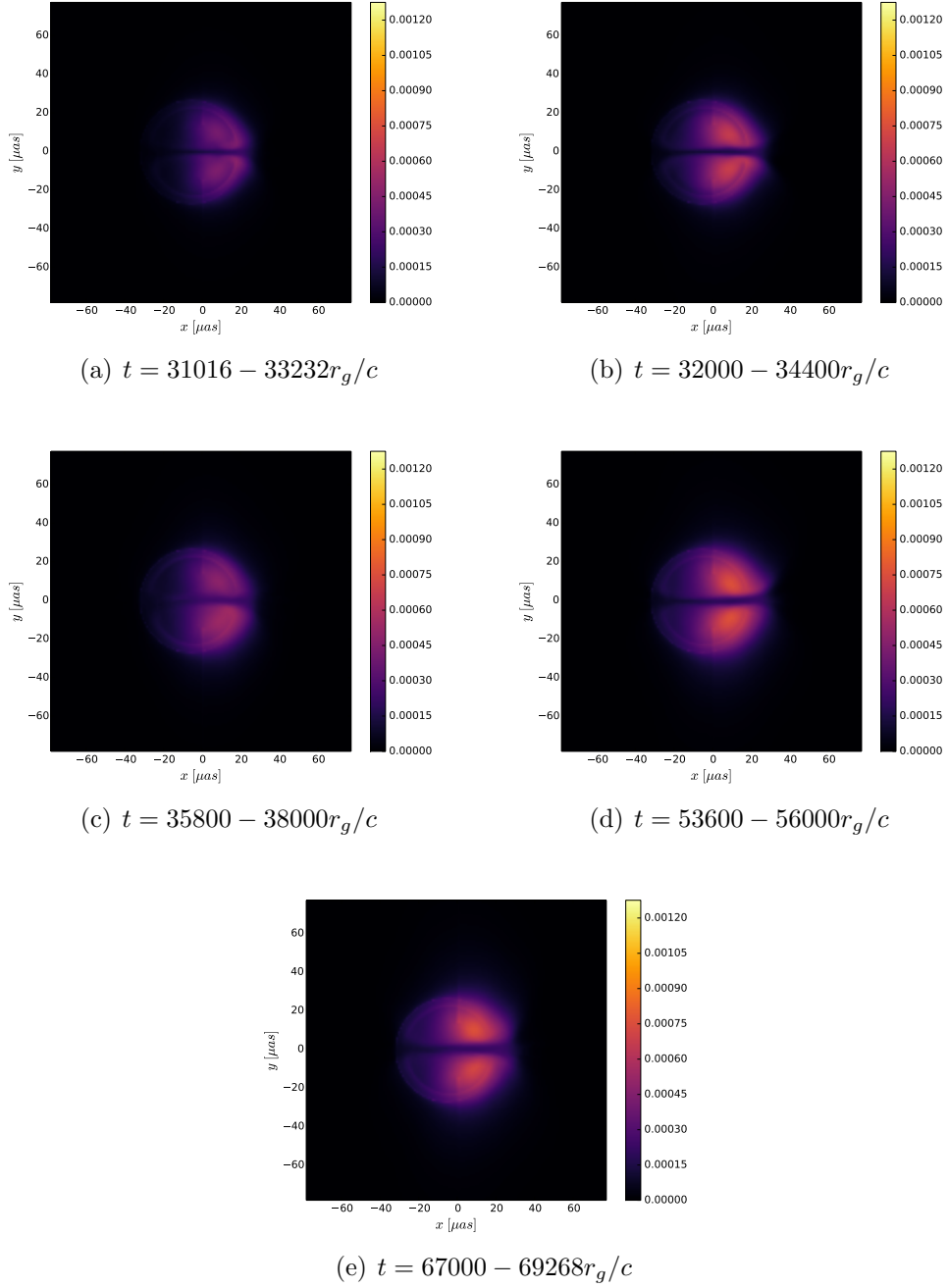
Figure 3.5: Simulated time-averaged intensity images for the edge-on case. The disk creates a void in the image, with the emission being most intense directly above and below it. Fig. 3.5(a) is the dimmest due to the magnetic RT event, while the periods with the highest average Υ have the highest average intensity.

(a) $t = 31016 - 33232 r_g/c$

(b) $t = 32000 - 34400 r_g/c$

(c) $t = 35800 - 38000 r_g/c$

(d) $t = 53600 - 56000 r_g/c$

(e) $t = 67000 - 69268 r_g/c$
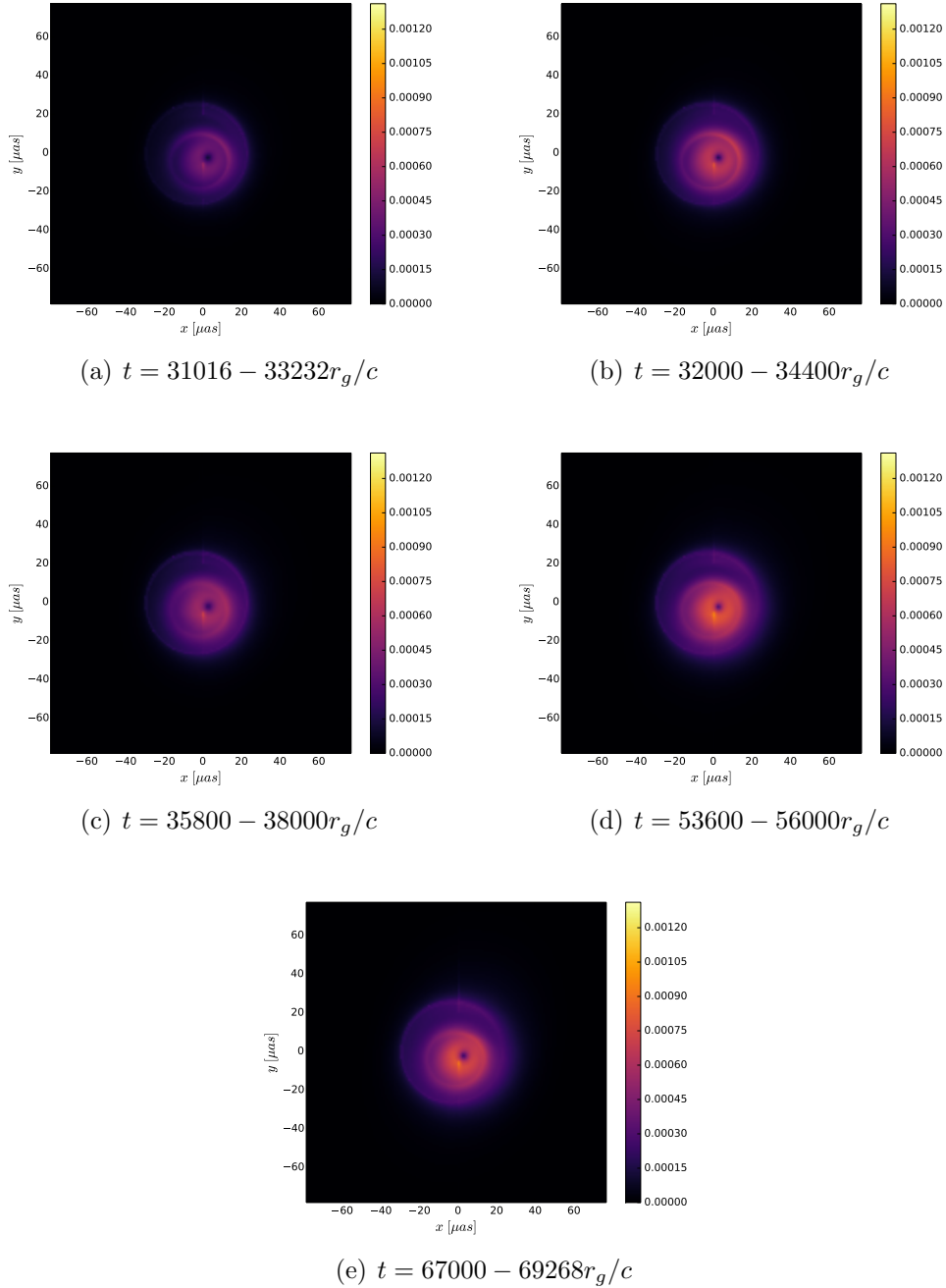
Figure 3.6: Simulated time-averaged intensity images for the tilted case. Fig. 3.6(a) is the dimmest due to the magnetic RT event, while the periods with the highest average Υ have the highest average intensity, in the edge-on orientation in Fig. 3.5.

(a) $t = 31016 - 33232 r_g/c$

(b) $t = 32000 - 34400 r_g/c$

(c) $t = 35800 - 38000 r_g/c$

(d) $t = 53600 - 56000 r_g/c$

(e) $t = 67000 - 69268 r_g/c$
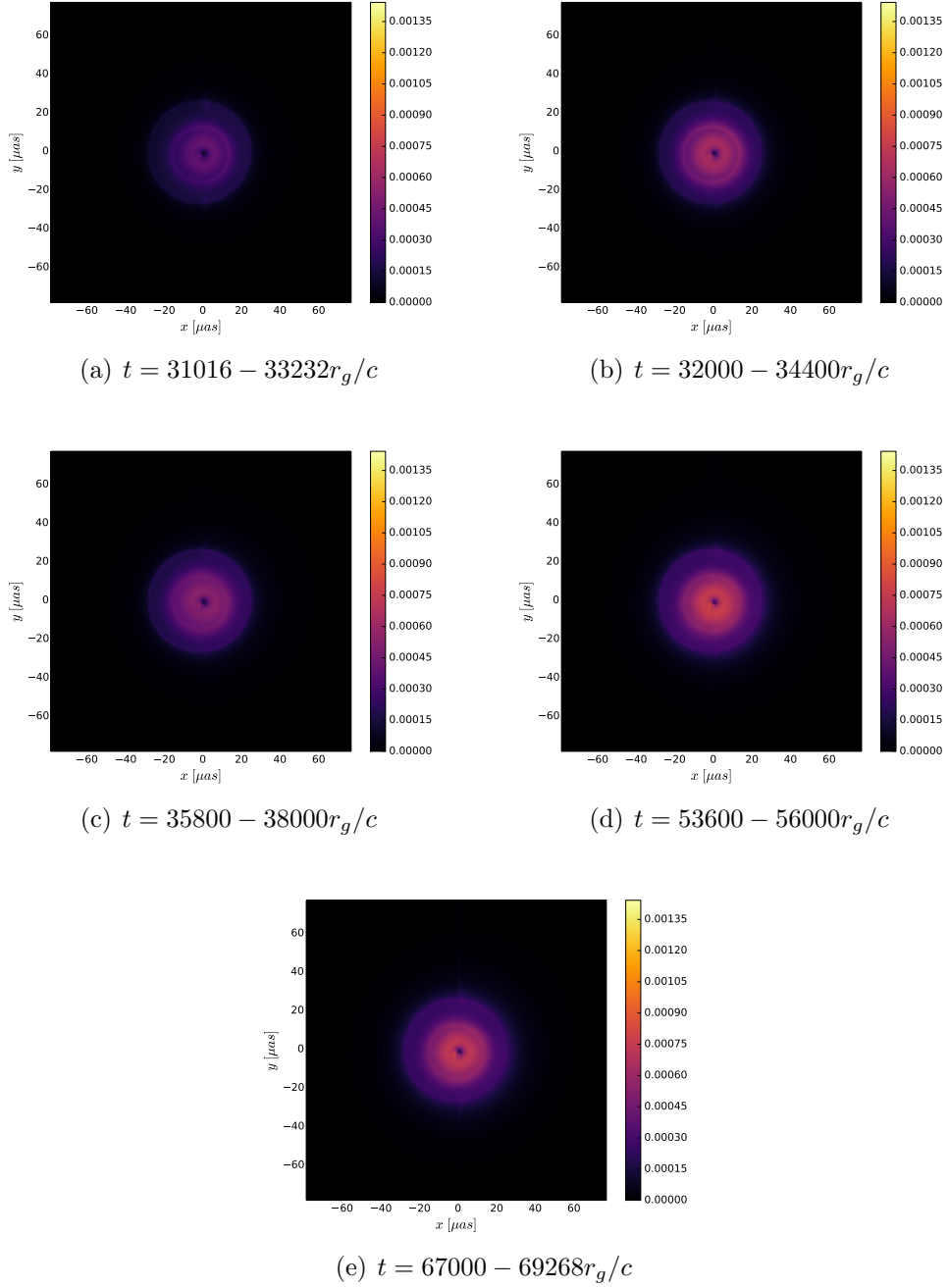
Figure 3.7: Simulated time-averaged intensity images for the face-on case. Fig. 3.7(a) is the dimmest due to the magnetic RT event, while the periods with the highest average Υ have the highest average intensity, in the edge-on orientation in Fig. 3.5.

reprocessed in the disk and pushed back onto the BH (Figs. 3.5(b), 3.6(b), and 3.7(b)), before dimming again slightly (Figs. 3.5(c), 3.6(c), and 3.7(c)). At the end of the simulation, when Υ_H is at its highest average value, the images also reach their highest intensity (Figs. 3.5(d), 3.6(d), 3.7(d), 3.5(e), 3.6(e), and 3.7(e)). Comparing the time-averaged intensity value, computed from the light curve data shown above, to the time-averaged Υ_H for each period show that there is a linear relationship between the two quantities. However, due to the broadened structure seen in Fig. 3.4, it does not seem like a causal relationship, but rather one with a third quantity driving both.

3.4.3 Intensity Snapshots

We also made snapshots of individual times to compare to the three-dimensional renderings of specific moments in the lifetime of the magnetic RT event (Fig 2.2 in Marshall et al. [1]).

In Figs. 3.8, 3.9, and 3.10, the effects of the expansion of the low density magnetic RT bubble are clearly seen. Particularly at times $t = 31164 r_g/c$ (Figs. 3.8(b), 3.9(b), and 3.10(b)) and $t = 31744 r_g/c$ (Figs. 3.8(c), 3.9(c), and 3.10(c)), the bubble creates a null spot in the image, which moves from the center close to the BH outwards as the bubble pushes into the higher density disk. After the bubble moves out to larger radii than shown here (Fig. 3.8(c), 3.9(c), and 3.10(c)) and begins to dissipate at $t = 32800 r_g/c$ (Figs. 3.8(d), 3.9(d), and 3.10(d)), the intensity becomes more equal across the whole image again.

(a) $t = 31016 r_g/c$

(b) $t = 31164 r_g/c$

(c) $t = 31744 r_g/c$

(d) $t = 32800 r_g/c$
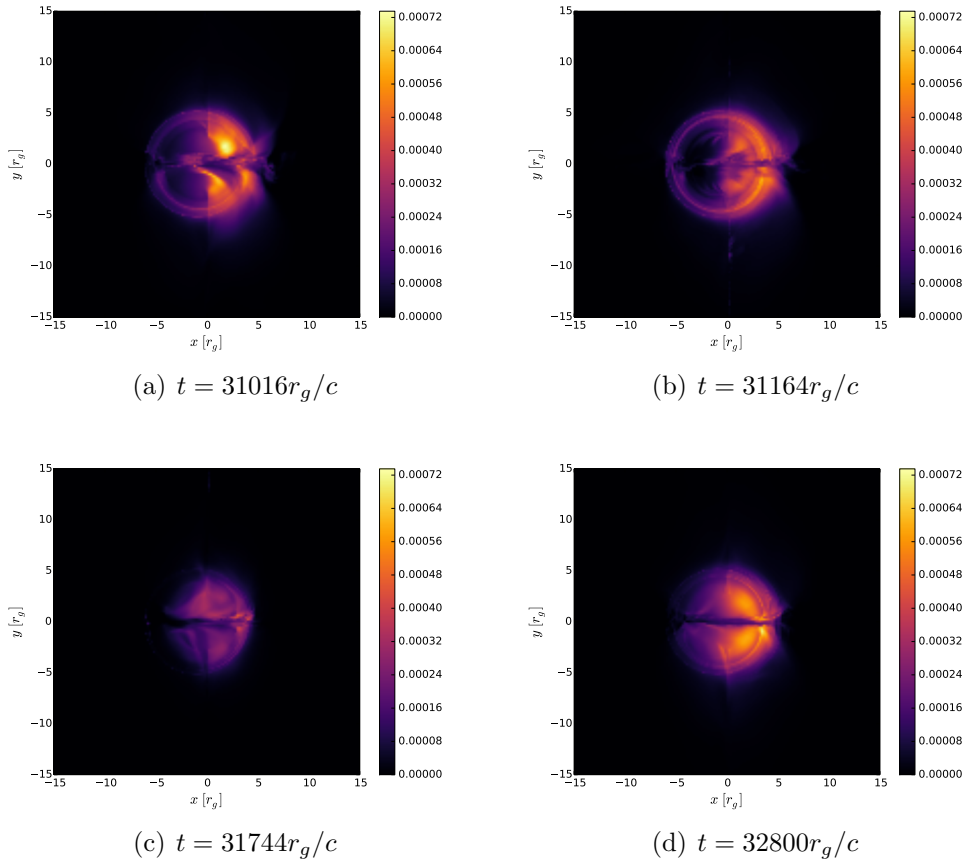
Figure 3.8: Simulated intensity snapshots for the edge-on case for the times shown in Marshall et al. [1] Fig. 2.2. In Fig. 3.8(a), the beginning of the disruption can be seen with flares above and below a void in the midplane. Fig. 3.8(b) shows the void created by the emergence of the magnetic RT bubble. After the bubble moves beyond the radius shown here (Fig. 3.8(c)), the void fills in even though the average intensity is lower than the previous time. In the final snapshot (Fig. 3.8(d)), the image has a more even and higher overall intensity, with a flare close to the disk midplane.

(a) $t = 31016r_g/c$

(b) $t = 31164r_g/c$

(c) $t = 31744r_g/c$

(d) $t = 32800r_g/c$
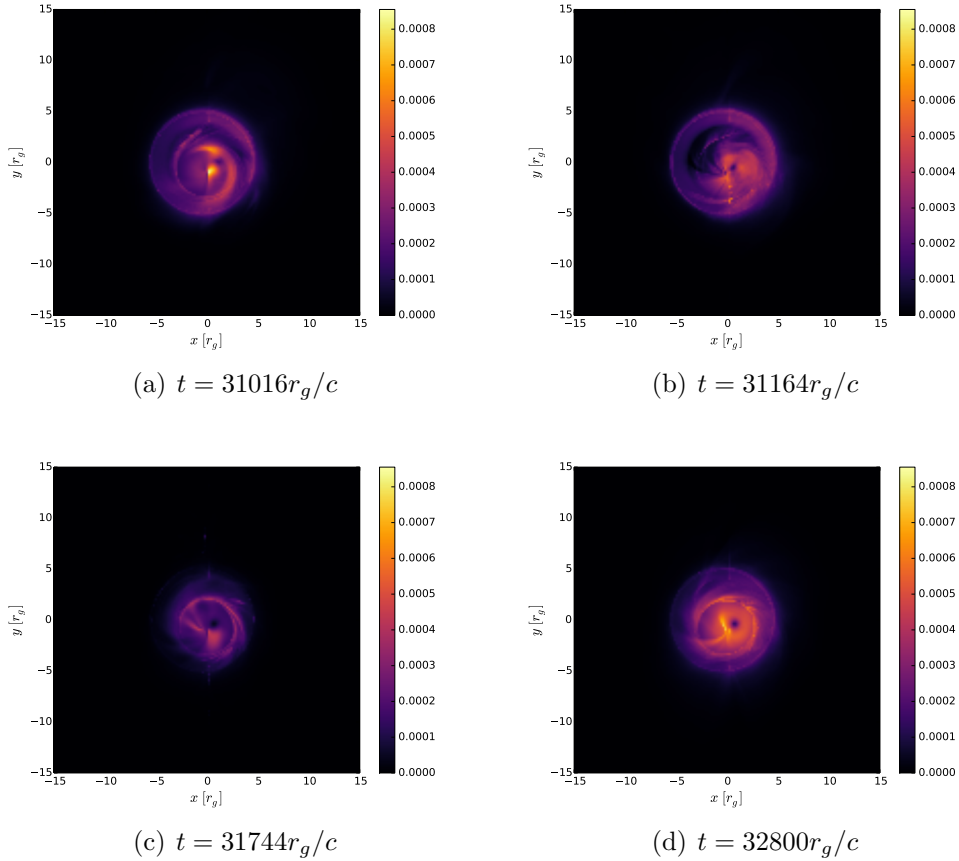
Figure 3.9: Simulated intensity snapshots for the tilted case for the times shown in Marshall et al. [1] Fig. 2.2. In Fig. 3.9(a), the beginning of the disruption is visible, though not as clearly seen as in the other orientations. Fig. 3.9(b) shows the void created as the magnetic RT bubble expands. After the bubble moves further outwards into the disk (Fig. 3.9(c)), the edges of the visible region are dimmed, with only a few filaments emitting. In the final snapshot (Fig. 3.9(d)), the image has a more even and higher overall intensity, with a flare close to center of the image.

(a) $t = 31016 r_g/c$

(b) $t = 31164 r_g/c$

(c) $t = 31744 r_g/c$

(d) $t = 32800 r_g/c$
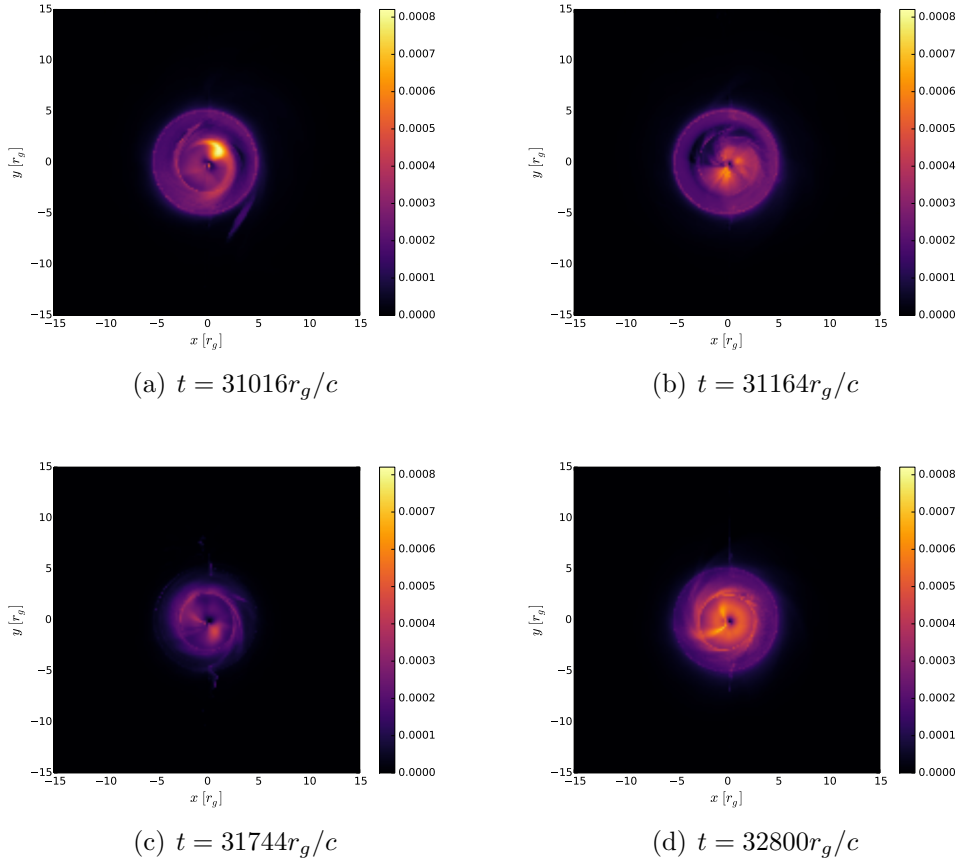
Figure 3.10: Simulated intensity snapshots for the nearly face-on case for the times shown in Marshall et al. [1] Fig. 2.2. In Fig. 3.10(a), the beginning of the disruption can be seen with a flare at the edge of the bubble. Fig. 3.10(b) shows the void created by the emergence of the magnetic RT bubble. After the bubble moves beyond the radius shown here (Fig. 3.10(c)), the edges of the visible region are dimmed, with only a few filaments emitting. In the final snapshot (Fig. 3.10(d)), the image has a more even and higher overall intensity, with a flare close to center of the image.

Another interesting feature is the bright spot in the image at $t = 31016r_g/c$ (Figs. 3.8(a), 3.9(a), and 3.10(a)). It is close to the BH and very near the disk midplane. This seems related to the higher density patches found at the edges of the emerging magnetic RT bubble, similar in appearance to the overdense hot spots studied in Broderick and Loeb [104, 105] and Doeleman et al. [106]. However, this bright spot is gone by the next snapshot at $t = 31164r_g/c \approx 1$ hour later when the low density region moves further into the disk, so it doesn't orbit the BH as the hot spots in those paper. Instead, it is similar to the streams formed by the injection of "clumpy matter" density perturbations found in Chan et al. [107].

3.5 Conclusion

In this work, we have shown that the magnetic flux on the BH, Υ_H, is closely tied to the luminosity at 230GHz using both the simulated light curves (Fig. 3.3) and the average intensity images. The nature of the relationship is undetermined, as the light curve structures are generally broader than the corresponding ones seen in Υ_H (Fig. 3.4), making it probable that there is another quantity, such as density, leading to this behavior in both I and Υ_H. We also note that the similarities between the simulated light curves at the three orientations considered in this work suggest that the observations are not greatly affected by the external variables such as viewing angle.

From the snapshots of the magnetic RT event (Figs. 3.8, 3.9, and 3.10), we see that the large low density bubble has a great effect on the observations,

from reducing the overall luminosity of the image to creating a void that could be detectable as a null by the EHT. There is also a flare in the luminosity at $t = 31016 r_g/c \approx 180$ hours close to the disk midplane at small radii that is likely an accreting packet of plasma.

Future work will include simulated scattering effects to more accurately depict what would be observed by the EHT. Gold et al. [86] describe a method for this that could be applied to the work presented here. As this would broaden the features observed, we would not expect the similarities between intensity images and the low density magnetic RT regions to be as clear, though still observable. We will also explore the polarization measurements also generated by ASTRORAY to search for more signs of the presence of the magnetic RT instability in SMBH accretion disks. Furthermore, we will generate synthetic observational data for other frequencies, particularly 345 GHz, which the EHT expects to observe at in the near future.

Chapter 4:   Structure of the Women in Physics Mentoring Program

4.1   Abstract

In this chapter, I will discuss the motivation for and structure of the UMD Women in Physics formal near-peer mentoring program. This program was started in Spring 2013 by Dr. Kristen Bursen to provide additional support to undergraduate women in the UMD physics department through relationships with older students. These older students would be able to offer advice on coursework, research, pursuing a graduate degree, and other topics relevant to the experience of women in physics. After Dr. Bursen's graduation, I took over as the mentoring coordinator, a position I have held since then. During the six years I have overseen the program, I have adapted it to better meet the needs of the students participating, incorporating elements from similar programs run through the Compass Project at the University of California Berkeley and Sundial Project at Arizona State University. Key changes include recruiting upper level undergraduate women as mentors, matching groups based on the mentee's preferences (speed matching), and partnering with the Astronomy Gentleladies' Network.

4.2 Introduction

Formal mentoring programs have been popular at universities for several decades, as they offer many benefits to the students involved in them, including improved retention rates [108, 109, 110, 111], academic performance [108, 110], and social connection [111, 112, 113, 114, 115, 116, 117]. These benefits are especially helpful for women in fields where they are underrepresented [118, 119, 120], such as physics. While women earn over half of all bachelor's degrees, only 21% of physics bachelor's degrees are earned by women [61]. This fraction has been consistent since 2007 after several decades of increase. Many efforts and programs have started to address this persistent gender gap, including mentoring programs. Seymour and Hewitt [119] found that women in science, technology, engineering and mathematics (STEM) are more satisfied in their major when they felt welcomed into the community and have more experienced role models, both of which are provided by mentoring programs. Whitten et al. [120] also describes mentoring as a part of the support found in female friendly physics departments.

In particular, peer and near-peer mentoring, where the mentors are closer in experience (and usually age) than more traditional mentoring relationships between faculty and undergraduates, has many additional benefits. First, using students as mentors provides a larger pool of potential mentors. In the case of same-gender mentoring for women, this broader pool reduces the pressure on the small number of female faculty members to serve as mentors to the female students in the department [111, 113, 121, 122]. Second, mentors closer in age and experience to their mentees

lessens the power differential between them, making peer mentors less intimidating and allowing the relationship to start on a more open and honest footing [113, 115, 122]. This makes the transition from role model to friend, an important source of support for underrepresented students [114, 123], easier.

Due to all of these benefits, a formal near-peer mentoring program was started for women in the University of Maryland Physics department in 2013. It was based on a component of the Compass Project at the University of California, Berkeley [124] and is similar to the Sundial Project mentoring program at Arizona State University [123]. In Section 4.3, I present a brief overview of the literature on mentoring. I then discuss the original format of the University of Maryland program in Section 4.4 and how it changed over the years to better meet the needs of the participants in Section 4.5. Finally, in Section 4.6, I present a summary of these changes and ideas to improve the program in the future.

4.3   A Brief Review of Mentoring Literature

In this section, I will describe the different ways researchers define and frame mentoring and the benefits it provides for the participants in mentoring programs. There are many definitions for what exactly mentoring entails, so a review of the literature will situate the style of mentoring practiced by the participants of the University of Maryland Women in Physics program. Finally, I will review some of the benefits gained from mentoring for both the mentees and mentors.

4.3.1 Definition and Model

In their reviews of mentoring studies, Jacobi [121] and Crisp [125] found over fifty different definitions of mentoring. While the many programs described in the literature lack a common definition, they share many common features to support students [126]. In particular, Jacobi [121] named fifteen different aspects of a mentoring relationship, which were grouped into four domains by Nora [110]: 1) psychological or emotional support, 2) role models, 3) goal setting and career paths, and 4) academic subject knowledge support. These were further reduced to "psychosocial support" (domains 1 and 2) and "academic support" (domains 3 and 4) by Zaniewski [123] and others. Since there are many other venues for students in the physics department to receive academic support (e.g. academic advisers, tutoring through the Society of Physics Students, etc.) and women's choices about entering a field of study have been shown to be influenced by their friend group [127, 128], the Women in Physics mentoring program primarily focuses on providing psychosocial support, though academic support is also provided. We therefore use a holistic model for mentoring that addresses both elements [113, 123, 129, 130].

Zaniewski [123] defines mentoring as "a dyadic platonic relationship between a more experienced student (mentor) and a less experienced student (mentee) at the same institution, with frequent, direct, face-to-face contact. Near-peer mentors ... provide guidance on academic and social issues, and help their mentees form a more robust institutional network." This is also the definition used by Women in Physics.

4.3.2 Sense of Belonging and Mentoring

Feeling a sense of belonging, defined by Lewis et al. as "...the extent to which students subjectively perceive that they are valued, accepted, and legitimate members...", in their chosen fields is an important factor in student success and persistence. Even aspects of life that are not focused on social interactions, such as physics or other academic pursuits, are affected by whether or not a person feels as if they belong. Many studies have shown that a lower sense of belonging is correlated with student attrition and that it has a greater effect on women than men. This is due in part to a lack of ingroup role models and peers lowering sense of belonging [117, 119, 127, 131].

Sense of belonging is closely tied to a student's identity as a scientist. This science identity can be framed as a composite of different yet interacting aspects: 1) personal identity, or how a student views themself, 2) social identity, how a student views themself as a member of a group, and 3) physics identity, how a student views themself relative to some archetypal physicist [132]. Each of these aspects can be targeted to improve a student's sense of belonging.

near-peer mentoring can increase belonging by acting on multiple of these areas. By providing role models with similar personal identities (e.g. both the mentor and mentee being women), the students' social identities are targeted and their belonging will increase. Dasgupta describes this function as "social inoculation" against stereotype threat and other factors that could lower belonging[127]. Dennehy and Dasgupta found that this protection against lowered belonging lasts

even after the mentoring relationship ends[111]. Social support and friendship also increase sense of belonging by affecting the social identity of the mentee [114, 131].

Additionally, Quan found that interactions with peers can lead to a more nuanced idea of the archetypal physicist (what she calls the normative identity), which leads to a stronger physics identity as the archetype and the student's personal identity become more aligned. In particular, she describes a case study of a student who progresses from a strict dichotomy between "smart" and "dumb" students, with the archetypal physicist being the former, to an understanding that everyone has strengths and weaknesses, including high achieving physics students [133]. In this way, mentors can affect the physics identity of the mentees, by providing examples of how to be a physicist that differ from the common stereotype and sharing their own struggles in the laboratory or classroom.

4.3.3   Benefits of Mentoring

While much of the mentoring literature is focused on the benefits for the mentees, near-peer programs are mutually beneficial for both the mentors and mentees [112, 134]. Here I summarize the primary benefits found in the literature.

4.3.3.1   Benefits to Mentees

In the literature evaluating the impact of mentoring programs on the undergraduate mentees, gains to both the academic and psychosocial domains are reported. In the academic realm, student participants' grades were significantly

higher than non-participants [108, 110, 125]. When Gunn et al. [134] surveyed first-year mentees in a peer mentoring program, academic support was the most reported benefit of the program, where they include support directly related to coursework (e.g. tutoring) as well as broader academic support (e.g. sharing campus resources, time management) in this category. Zaniewski and Reinhold also find a similar distribution of topics discussed in their evaluation of the Sundial mentoring program [123]. Another benefit of mentoring is helping students set goals for their careers, including plans to earn advanced degrees [111, 134]. Mentoring also improves retention of students involved [108, 109, 110, 111].

Emotional support was the most commonly reported benefit in the psychosocial domain [134]. Students connect with older students who act as role models and advisers [111, 112, 113, 134], creating a space for students to discuss concerns that don't fit in more academic focused contexts [123]. Frequently, these relationships evolve into friendships, a key factor in retaining underrepresented students [119, 123], and this social connection help reduce stress for the mentees [112, 114, 115]. Additionally, many of these effects were found to persist a year after the mentoring relationships ended [111].

4.3.3.2   Benefits to Mentors

In addition to all the benefits to the mentees in near-peer mentoring programs, mentors also gain from their participation. Studies of the effects of mentoring on mentors report mentors feeling more engaged with the community and improvements

to their self-confidence, communication skills, and leadership abilities through acting as a role model [113, 115, 134, 135, 136]. Mentors also gain a sense of pride from helping support younger students [137]. In addition, these studies find that mentors report improved academic skills as well, but due to the difference in population of the mentors (predominantly graduate students in the WiP program; undergraduate students in these studies) and structures of programs described, these might not be found in the UMD WiP program.

4.4 Overview of the Women in Physics Mentoring Program

The Women in Physics mentoring program has a formal near-peer structure, where mentors are assigned to mentees. This structure was chosen since formal mentor programs explicitly bring students into community and networks they might not otherwise become a part of, as mentioned above. Students join the program by completing an application, the answers of which are used to match mentors with mentees. After the mentor-mentee dyads are assigned, they are asked to meet three times each semester (approximately monthly). At the end of the semester, a survey with both open-ended and Likert scale questions is administered to assess the program.

Over the years, while this underlying structure has stayed the same, I have made significant changes to certain elements of the program. When the program began, the groups were pairs with a single graduate student mentoring a single undergraduate student. These pairs were matched primarily based on research in-

terests. Neither the mentors nor mentees had any training to establish what was expected as a participant in the program. There was no enforcement or incentive to ensure pairs met the requested number of times. In the following section, I describe how I have changed these areas of the program to better meet the needs of the participants, as well as the partnership with AGN this past year. In Appendix A, I include the original application and end of semester evaluation and in Appendix B, the current application, training materials, and both the individual meeting and end-of-semester surveys. While these changes have been made iteratively, I only included this year's materials for brevity.

4.5 Iterations and Improvements

4.5.1 Group Structure

Over the years, many changes have been made to the mentoring pairs. Originally, the mentoring relationship was one graduate student with one undergraduate. Since then, the structure has changed to include small groups and mentoring "chains", where a graduate student mentors an advanced undergraduate student who is mentoring a younger undergraduate, as well as one-on-one pairs.

The pairs were expanded into groups initially due to an imbalance in the number of mentors and mentees. With their permission, some of the graduate students were given two mentees. The meeting arrangements were left up to the group, who could choose to meet all together or have several one-on-one meetings, as long as the mentor met with each mentee at least three times as the program

requires. Groups also give younger students multiple connections to the physics department community, helping them integrate socially.

The mentoring chain was an idea that came out of my experience trying to mentor two undergraduate women during the 2016-2017 school year. I noticed that I had fewer answers for the first year student I was mentoring than the other student did, since I didn't have as much UMD-specific knowledge, such as information about on-campus housing, interesting courses to fulfill general education requirements, or the structure of various math courses. As Gershenfeld discusses, freshmen have different needs than seniors and therefore need different support from their mentors [126]. The following year, senior undergraduate students were recruited as mentors for the youngest mentee applicants, while the senior women were assigned graduate student mentors. This gave both the younger and older undergraduates mentors with the knowledge they most needed and multiple role models at different points of their career for the younger student. In addition to providing mentors with more institution specific knowledge, adding undergraduates to the pool of mentors increased the number of mentors available and making it less necessary to have larger groups.

4.5.2 Matching

As a formal mentoring program, the participants are assigned partners. While this has the benefit of connecting students with a network and support they might not have access to through informal relationships, the mentee only benefits if a strong

connection to the mentor is built. It is therefore important to assign pairs that have common interests. To that end, participants join the program by completing a brief application sharing their research and personal interests and these responses are used in matching. Originally, only the application responses were considered in the matching process, but more recently, mentors and mentees have been given the opportunity to meet with each other and share their preferred partners.

4.5.2.1 Application Only

From the program's beginning in 2013 through 2017, mentors and mentees were matched using their responses to the application and any personal knowledge I had of the applicants. The application was modified through the years to provide more information for the matching process and the preferences of the applicants. Key additions include asking about hobbies, so that the pairs could be formed based on shared activities in addition to physics interests, and what the applicant wished to gain through the program (advice on specific topics, friendship, etc.). Also, participants were given more control over their matching, through questions about what aspect they should be matched based on (research interest, hobbies, or other things to gain from the program) and the size of the group they are in. Finally, if the applicant has been a participant in the mentoring program previously, they are able to request the mentor/mentee they were matched with before.

Once the application period ends, the first assignments made are those who requested the same mentor/mentee from the previous year. If they have chosen not

to be part of a group, they are then removed from the pool of potential matches; otherwise, the mentors are still considered as matches for other mentees. After this, the applicants are sorted based on how they chose to be matched and pairs are assigned based on the similarities of their responses. Frequently, I know the applicants and use my knowledge of their personalities to create groups that I believe are likely to get along. This is helpful as one of the main problems for the program is pairs not meeting enough over the semester and pairs that have more to talk about seem more likely to meet often.

4.5.2.2 Speed Matching

While I make every attempt to match mentors and mentees who have multiple things in common and I believe will build a strong mentoring relationship, there are group assignments that do not meet often enough. This is one of the weaknesses of formal mentoring programs, as lack of mentor/mentee choice can reduce interest in the partnership [121]. To improve the likelihood of good matches, Anna Zaniewski, who runs the Sundial mentoring program, suggested a new component to the matching process that is used in the Sundial program, where program participants have the opportunity to meet many possible partners and express preferences on their matching assignment [123, 138, 139].

For the 2017 and 2018 cohorts, this "speed matching" event was held before the group assignments were made, where the potential mentors and mentees are able to meet and talk to one another. It was one hour long, with snacks to promote

a more social attitude, as suggested in Zaniewski [123]. To enhance this casual attitude, the two events have been held on Friday afternoons. At the event, mentors and mentees were arranged in concentric circles facing one another. They spoke with the person across from them for a brief period of time (3-5 minutes, depending on the number of attendees) before rotating to speak to a different potential partner. The senior undergraduate students who applied as both mentors and mentees complicated this set up, as they need to speak to both groups. Many of these students had been mentees the previous year and wanted to be matched with the same mentor, therefore they only needed to meet the youngest mentees and were just a part of the mentor circle. The rest of them choose which relationship they want to prioritize and join the appropriate group (e.g. a senior might feel it is most important to find a good mentor to help with graduate school applications and would then join the mentee group.) At the end of the event, the attendees listed their top three choices for their mentor/mentee.

Since it is unlikely everyone will attend, I share the application responses with their potential matches after removing any private comments so that the attendees can learn about possible partners who aren't there. This also allows those who don't attend to get a sense of who they would prefer to be matched with. I ask those who don't attend to email me their top three choices. I also ask the upper level undergraduates who applied as both mentors and mentees to do the same whichever group they didn't get to interact with at the event (e.g. for the senior in the example above, she would email her choices for a younger undergraduate to mentor).

Once all the participants have stated their preferences, matching begins. As with the application-only matching method, the first step is to match any pairs or groups from the previous year that have requested to be re-matched. After this, the student preferences are considered and any pairs that select one another as their top choice are assigned. From there, I consider any matches in second and third choices and try to assign pairs from those. This continues until everyone is assigned to a pair or group. In the case that there are multiple potential pairs based on the student preferences, I will use any knowledge I have of the participants and the similarity of their application responses to assign pairs who have common interests.

In addition to adding an element of participant choice to the matching process, the speed matching event also provides a venue for the mentors and mentees to meet, making the initial foundation of the relationship stronger than when the applicants are matched with a stranger.

4.5.3 Training and Support

For the first time in 2018, I held an information and training session for potential mentors. Previously, I distributed guides I created describing the program requirements, suggestions for activities, and a list of campus resources. The training started with a group discussion about the different styles of mentoring [113, 126, 140] and what contributes to a successful mentoring relationship. It also included role-playing hypothetical scenarios adapted from the American Physical Society (APS) Physics Research Mentor Training [141] (specifically the scenarios on pages 25, 61,

and 71), and reviewing the previous years' documents. The discussion questions and mentoring guidelines can be found in Appendix B.

Since there are so many roles that a mentor can take, it is important for each pair or group to identify and communicate their own expectations from the relationship [126, 140]. To facilitate this, I created and distributed a Mentoring Expectations Agreement statement (see Appendix B) for the groups to discuss during their first meeting. The discussion prompts it contains form an explicit groundwork for the relationship and clarify how the group will operate as they meet through the year.

4.5.4 Incentivizing Requirement Fulfillment

Another method I have used to ensure that mentoring groups are successful and meet as frequently as they should, in addition to incorporating student choice in the matching process, is to offer $5.00 Terrapin Express Dining Cards to the participants who attend and report at least two meetings each semester (for more details on the meeting status report, see discussion in section 4.5.5). This also helps offset the costs of the meetings, which frequently occur over a meal or coffee, for the participants, though this would be more effective if the gift cards were given at the beginning of the semester, not the end.

4.5.5 Assessment and Feedback

As a means of prompting the participants to reflect on the effects of the program and solicit suggestions for improvements, I administer several different surveys over the course of the year. The surveys also allow me to monitor how the groups are faring and if there are any problems I need to address.

First, there is the short status report the participants are asked to respond to after each meeting. This survey asks about the activities done and topics discussed, as well as how well the pairing is working. This last component is particularly important, so that if any pair are incompatible, they can be reassigned without losing significant time and chances to meet with a more compatible mentor/mentee. Since the participants can meet anytime during the semester, I check the response monthly to see if anyone reported any issues and to track how often pairs have met, in order to distribute the Terrapin Express cards, as discussed above.

Second, there is the Fall semester survey, which is a slightly longer survey to probe more in depth how the semester went, if the program is helpful, and if any changes need to be made in the groups. The fall semester survey is primarily to uncover any poorly functioning groups who either haven't met or haven't responded to the meeting report. It is more focused on whether there have been meetings and if the group is getting along than the details about individual meetings asked about in the status report.

Finally, the end-of-year survey is the longest survey, based off of the culminating survey from ASUs Sundial mentoring program [139]. This survey solicits

feedback on how the program is run, how the individual felt about the program, and if they thought it was helpful. This is the most important survey for evaluating the effectiveness of the program and what changes need to be made moving forward. It has questions about how the group functioned over the year, if the program was beneficial, and suggestions for improving the program in the future. To ensure most, if not all, the participants respond, I email each participant individually to ask them to share their thoughts, rather than an email to the whole group that is easier to ignore, another suggestion from Zaniewski [138].

4.5.6 Partnership with Astronomy Gentleladies' Network

In 2018, during a discussion with the AGN officers about possibly planning joint events with WiP, it was mentioned that AGN was interested in providing mentoring for the undergraduate women in the astronomy department. Rather than build their own program, we decided to collaborate. This broadened the pool of participants, greatly increasing the number of mentors in the program. Also, the increase in leadership of the program allowed for training to be planned and offered for the first time.

4.6 Conclusion and Outlook

In order to provide extra community and support to the undergraduate women of the physics department, attributes that contribute to increased retention and other benefits, a formal near-peer mentoring program was started by WiP. In the

years since, the program has grown by expanding the pool of possible mentors to include advanced undergraduate women, improved the matching method so the groups are more likely to build strong relationships, and providing compensation for the participants' efforts. WiP also partnered with AGN this past year to expand the program to the astronomy department, a collaboration which allowed mentor training to be provided for the first time.

There are several additions that could be made to the program further develop in the future. First, to make meeting easier for the pairs, I think a regular newsletter with relevant campus events (such as a WiP Professional Development Luncheon or interesting seminars) would be helpful. Mentoring program specific social events could be also held to provide additional opportunities for pairs to meet and would also give participants a chance to interact with the broader program community, rather than their own small group. I also think a longer mentor training session would be helpful, to allow more time for discussion and more material to be covered. This would also provide an opportunity to build even more community in the department, as the mentors would get to know one another more. Mentee training could also be added, though there are very few resources available that could be used. Finally, regular meetings with all of the mentors would also be helpful to the program. They could discuss challenges they were facing, share ideas to address them, and get to know one another better, another way to build more community. A similar meeting for just the mentees would also be beneficial.

Appendix A: 2013 Mentoring Documents

A.1   Program Application

- Name

- I am a:

  - graduate student

  - undergraduate student

- Year

- Email address

- Why do you want to be part of the mentoring program?

- How often are you interested in meeting with your mentoring partner(s):(check all that apply)

  - Every week

  - Every other week

  - Once a month

- GRADUATE STUDENTS: I would be heartbroken if I didnt get paired with someone due to lack of undergrads...

  - Yes

  - No

- GRADUATE STUDENTS: What is your sub-field?

- UNDERGRADUATE STUDENTS: What are you thinking about doing after college? Are you considering graduate school? If so, do you have particular sub-field(s) of interest? What?

A.2 End of Semester Survey

- Likert scale questions

  - I benefited from my interactions with my mentor/mentee

  - My mentor/mentee was a good match for me

  - I am interested in being in the program next semester

  - I would recommend this program to a friend

- Open response Questions

  - What did you like about the program?

  - What suggestions do you have for improving the program?

  - Any suggestions for activities?

  - Do you have any other comments or suggestions about the program?

Appendix B: Fall 2018 Mentoring Documents

B.1   Program Application

- Name

- Email Address

- What department are you a part of?

- Research Field/Area of Interest

- Are you applying to be a mentor or mentee?

- Year/Class

- How often would you like to meet with your partner?

    - Weekly

    - Twice a month

    - Monthly

- (Mentors) What do you feel you can offer your mentee? (Mentees) What would you like to gain from the program?

    - Academic support

    - Research advice

    - Grad school tips

    - Life outside academia

    - General life tips

    - Friendship and community

    - Other

- What are your hobbies and interests?

    - Outdoorsy things

    - Games

    - Food and drink

    - Movies

    - Musics

    - Sports

    - Other

- How would you like to be matched with your mentor/mentee?

  - What to get from the program

  - Research area

  - Hobbies

- Would you want to be in a group?

  - Yes

  - No

  - Doesn't matter

- If you were in the program last year, who was your mentor/mentee? [1]

- If you participated in the program last year, would you like to keep the same pairing? [1]

- Is there anything else you would like potential matches to know?

- Additional private comments [1]

B.2 Training Documents

B.2.1 Discussion Questions

- What kinds of mentoring have you experience? What kinds of ways have you mentored? (in a general sense)

---

[1]Responses to these questions were kept private, rather than included in the speed matching information

- What are some factors and attributes of successful mentoring relationship? (smaller details)

- How can you balance giving mentees direct support while helping them maintain/foster their independence?

- What do you think is/will be the biggest challenges in mentoring? How would you address it?

- What kinds of resources do you use in mentoring?

B.2.2   Mentoring Suggestion and Campus Resource Guide

Women in Physics and Astronomy Gentleladies' Network Mentoring Program Suggestions

Suggestions Adapted from materials from the Compass Project and the Sundial Project

- Take an active, interested role in the relationship. Being "approachable is not enough. Mentors need to proactively ask questions and check in with their mentees.

- Communicate frequently. Especially early on in a relationship, frequent (even brief) check-ins help to develop trust, rapport, and identify issues the mentee is struggling with

- Meet with your mentee on a regular basis. Being consistent will not only foster trust, it will avoid damaging the relationship should you or your mentee

83

have to cancel on occasion. Establishing a regular schedule is a great item to discuss when you first meet.

- Find a place to meet that is not distracting and noisy. Meet in a public place, preferably one that is frequented by other students.

- Define clear expectations and boundaries from the very beginning. Be sure to ask about your mentees expectations. As a starting point, you can go over the Mentoring Expectation Discussion Prompts during an early meeting.

- If you are meeting with your mentee infrequently, please be sure to communicate that you are available should the need arise and check in on a regular basis. You can also try suggesting a meeting with a specific topic (picking classes for the next semester, finding an REU, etc.) to discuss. If your mentee wants or needs a mentoring relationship that is more active than you can provide, refer them to additional resources offered through the school (see Campus Resource list).

- If your mentee is hesitant or inconsistent in contacting you, continue to make a regular effort to build the relationship. Try many avenues of communication, even social media (Facebooks read message notification might increase your chances of getting a response!). If this is a persistent problem, please let me know and I'll try to help.

- Share some of your own relevant stories and experiences. Dont be concerned about knowing everything they need or having the best advice, but share what

you can.

- Offer encouragement in both good times and bad. Be aware of signs of stress from your mentee and of the difference between what is normal and what would require more attention. Is your mentee becoming frustrated by things outside of the purview of your normal rapport?

- Listen actively. Ask questions that open a dialog and follow-up questions. Show interest in your student.

- Demonstrate both faith in the abilities of your student and high expectations for their success. One without the other can be detrimental to students motivation. Celebrate accomplishments. Express enthusiasm for when your student succeeds.

- Be aware that all students do not share the same access to academic networks. It is important to ask questions before assuming that your mentee is aware of a resource or skill that may come as second nature to you.

Possible Discussion Topics

- Professional

  - Goals, skills and interests

  - Time management

  - Study habits

  - Feeling overwhelmed/doubting ones abilities/impostor syndrome

- This discussion is better after trust has been established

- Expectations of your school, department and major

- Job or career expectations

- Personal

  - Work and school experiences

  - Why you both chose your college

  - How to develop a sense of belonging

  - Maintaining a healthy lifestyle

  - Favorite television shows or movies

  - Sports and hobbies, both indoor and outdoor

Possible Activities

- On campus

  - Coffee or lunch, particularly AGN tea times (Payday Fridays at 4 pm) and WiP Professional Development Luncheons (TBA)

  - Taking a walk

  - Visiting the farm

- Off campus

  - Cooking or baking together

  - Watch a movie

- Visit the Smithsonians

- Manicures

- Go to the Women in Physics Monthly Social Event

- Hiking, ice skating or other sport/physical activities

- Games at Board and Brew

Campus Resources

- The Writing Center

- Tutoring

  - University tutoring

  - Society of Physics Student drop-in tutoring

  - Student tutors in the Astronomy Undergraduate Interaction Room

- Learning Assistance provides workshops on a range of topics such as time management and test anxiety and offers academic counseling

- On campus counseling services

  - Behavioral Health Center

  - Counseling Center (also offers some academic resources)

  - Center for Healthy Families

- LGBTQ+ Resources

  - LGBT Equity Center

– Out in STEM and other student groups

- Departmental Resources - For issues more closely related to coursework or research, here are the people to talk to in each department

  – Physics Office of Student and Education Service, particularly Donna Hammer

  – Dr. Hayes-Gerhkey, Astronomy Department academic advisor

B.3   Expectations Agreement

As you start meeting with your mentor/mentee, its best to start with a clear understanding of what you both expect from the relationship. To help establish this, here are some guidelines and questions to discuss during your first meeting.

Guidelines (Taken from materials from Arizona State Universitys Sundial Program [139])

A mentor is:

- A guide with experience and knowledge who is committed to the mutual growth of the mentor and mentee

- A caring facilitator who helps their mentee make use of resources and increase their network

- A trusted ally and advocate who works on behalf of their mentees best interests

- Sets high expectations and has a high level of belief in the capabilities of their mentee

A mentor is not:

- A (surrogate) parent

- A professional counselor or therapist

- A trained tutor

- A romantic partner

- Judgmental

- Given to gossip

As a mentor, you agree to:

- Not discriminate against your mentee based on religion, national origin, ethnic heritage, race, sexual orientation, sexual identity, or disability.

- Respect the values of your student mentees and his/her family members

- If you have issues with your mentoring group, you will contact the program leaders.

- Understand your limits and refer your mentee to resources where appropriate (e.g. mental health resources).

- Respect the confidences of your mentee, and ask their permission before disclosing your conversations to others (except as required by the UMD student code of conduct, including your responsibilities as a mandatory reporter).

- Abide by UMD student code of conduct.

As a mentee, you agree to:

- Proactively communicate with your mentoring groups.

- If you have a concern about your mentoring group, contact the program leaders.

- Understand your mentors limits. If they offer to study with you, great, but dont expect them to be a substitute for a tutor.

- Not discriminate against anyone in your mentoring group based on religion, national origin, ethnic heritage, race, sexual orientation, sexual identity, or disability.

- Respect the confidences of your meetings, and ask permission from all members before disclosing personal conversations to others (exception: alerting the program leaders or appropriate UMD staff about specific concerns).

- Abide by the university code of conduct.

Questions

- How often will you meet this semester?

- What is the best way to contact you?

- What topics will the relationship focus on (schoolwork, research, general life issues, etc.)? Generally describe what you hope to gain from the relationship.

- What (if any) are the short term goals for the relationship?

- What (if any) are the long term goals?

- How will we deal with confidential information?

- Any other topics that we should discuss?

B.4   Meeting Status Report

- Name

- Who did you meet with?

- Date of the meeting

- What did you do during the meeting?

- Which of the following topics did you talk about?

    - Coursework

    - Research

    - Employment options/opportunities (short term)

    - Employment options/opportunities (long term)

- – Personal lives

- – Time management

- – Organization

- – Social and/or cultural issues

- – Other:

- How is your mentor/mentee doing?

- Are you getting along with your mentor/mentee?

- Do you have any concerns about your meeting? For example if you do not have good rapport, if you feel uncomfortable with them as a mentee/mentor, if there is something in the mentee/mentor's behavior that concerns you. This response will not be shared with your mentee/mentor.

  - – Yes, I have concerns

  - – No, everything is fine

- If yes, what is the nature of your concern?

- Additional Comments

B.5 Fall Semester Survey

- Name

- Are you a mentor or mentee?

- Who are you paired with?

- How well did you get along with your mentor/mentee this semester?

- How many times have you met this semester?

- Please describe what a typical meeting was like in your group

- If you haven't met at least 3 times, why not?

- How much have you benefited from your relationship with your mentor/mentee? (Likert scale question from "Not at all" to "Very much")

- If you have benefitted, how?

- Have you attended any of the large group events? This includes Women in Physics socials, study hour, and Professional Development Luncheons

- If you've been to a large group event, which one(s) and did you enjoy it?

- What do you like about the program?

- What suggestions do you have for improving the program next semester?

- Additional Comments

B.6 End of Year Survey

- Name

- Who were you paired with? [2]

---

[2]Participants in groups or chains were asked to complete the survey once for each person they met with.

- Are you a mentor or mentee?

- How many times have you met with your mentor/mentee this year?

- If you haven't met at least 3 times each semester, why not?

- How well do you get along with your mentor/mentee?

    - Very poorly

    - Poorly

    - Neutral

    - Well

    - Very Well

    - Other

- What kinds of activities did you do with your mentor/mentee?

    - Academic

    - Networking

    - Non-academic enrichment

    - Social

    - Other

- What topics did you discuss during your meetings with your mentor/mentee?

    - Coursework

– Research

  – Employment options/opportunities (short term)

  – Employment options/opportunities (long term)

  – Personal lives

  – Time management

  – Organization

  – Social and/or cultural issues

  – Other

- Please complete the following sentence: "Through the mentoring program, I've..."

  – bonded with someone else in STEM

  – connected more with the WiP and/or AGN community

  – met new people in STEM

  – Other

- Have you attended any WiP or AGN events that were not specific to the mentoring program?

- In what ways has the mentoring program contributed to you geeling more connected to the WiP and/or AGN community? In what ways has it not?

- What do you like about the program?

- Did any topics or issues come up that you would want training on to have a more effective mentoring relationship in the future? If so, what?

- What suggestions do you have for improving the program next year?

- If you will be in College Park over the summer, would you like to have another group event?

- Additional comments

- Mentor-only Questions

  - Do you feel like you have benefited from your relationship with your mentee? (Likert scale question from "Not at all" to "Very much")

  - How have you benefited from the program and your relationship? Why do you invest your time in mentoring?

  - Were any of the materials presented at the training useful? If so, which?

- Mentee-only Questions

  - How much have you benefited from your relationship with your mentor, in each of the following ways: (Likert scale question from "Not at all" to "Very much")

    * Academically

    * Increased sense of belonging

    * Stronger support network

    * Overall

– Please expand on any of your answers above about the benefits of your mentoring relationship

– Please describe a time your mentor helped you

– Please finish the following sentence: "Through conversations with my mentor, I've learned..."

  * that everyone struggles with STEM

  * that I am not alone in questioning whether I belong in STEM

  * about impostor syndrome

  * to recognize when impostor syndrome is impacting me

  * to talk openly about failures and setbacks

  * Other:

Bibliography

[1] Megan D. Marshall, Mark J. Avara, and Jonathan C. McKinney. Angular momentum transport in thin magnetically arrested discs. *MNRAS*, 478(2): 1837–1843, Aug 2018. doi: 10.1093/mnras/sty1184.

[2] K. Schwarzschild. On the Gravitational Field of a Mass Point According to Einstein's Theory. *Abh. Konigl. Preuss. Akad. Wissenschaften Jahre 1906,92, Berlin,1907*, 1916:189–196, Jan 1916.

[3] Albert Einstein. Die Feldgleichungen der Gravitation. *Sitzungsberichte der Königlich Preußischen Akademie der Wissenschaften (Berlin*, pages 844–847, Jan 1915.

[4] Julian H. Krolik. *Active galactic nuclei : from the central black hole to the galactic environment*. 1999.

[5] P. Padovani, D. M. Alexander, R. J. Assef, B. De Marco, P. Giommi, R. C. Hickox, G. T. Richards, V. Smolčić, E. Hatziminaoglou, and V. Mainieri. Active galactic nuclei: what's in a name? *A&ARv*, 25(1):2, Aug 2017. doi: 10.1007/s00159-017-0102-9.

[6] Carl K. Seyfert. Nuclear Emission in Spiral Nebulae. *ApJ*, 97:28, Jan 1943. doi: 10.1086/144488.

[7] W. Baade and R. Minkowski. On the Identification of Radio Sources. *ApJ*, 119:215, Jan 1954. doi: 10.1086/145813.

[8] L. Woltjer. Emission Nuclei in Galaxies. *ApJ*, 130:38, Jul 1959. doi: 10.1086/ 146694.

[9] M. Schmidt. 3C 273 : A Star-Like Object with Large Red-Shift. *Nature*, 197 (4872):1040, Mar 1963. doi: 10.1038/1971040a0.

[10] Ya. B. Zel'dovich. The Fate of a Star and the Evolution of Gravitational Energy Upon Accretion. *Soviet Physics Doklady*, 9:195, Sep 1964.

[11] E. E. Salpeter. Accretion of Interstellar Matter by Massive Objects. *ApJ*, 140: 796–800, Aug 1964. doi: 10.1086/147973.

[12] H. Bondi. On spherically symmetrical accretion. *MNRAS*, 112:195, Jan 1952. doi: 10.1093/mnras/112.2.195.

[13] Jonathan C. McKinney, Alexander Tchekhovskoy, Aleksander Sadowski, and Ramesh Narayan. Three-dimensional general relativistic radiation magneto-hydrodynamical simulation of super-Eddington accretion, using a new code HARMRAD with M1 closure. *MNRAS*, 441(4):3177–3208, Jul 2014. doi: 10.1093/mnras/stu762.

[14] N. I. Shakura and R. A. Sunyaev. Black holes in binary systems. Observational appearance. *A&A*, 24:337–355, 1973.

[15] I. D. Novikov and K. S. Thorne. Astrophysics of black holes. In *Black Holes (Les Astres Occlus)*, pages 343–450, Jan 1973.

[16] R. P. Kerr and A. Schild. A new class of vacuum solutions of the Einstein field equations. In *IV Centenario Della Nascita di Galileo Galilei, 1564-1964*, page 222, Jan 1965.

[17] R. P. Kerr and A. Schild. Republication of: A new class of vacuum solutions of the Einstein field equations. *General Relativity and Gravitation*, 41(10): 2485–2499, Oct 2009. doi: 10.1007/s10714-009-0857-z.

[18] Anuradha Koratkar and Omer Blaes. The Ultraviolet and Optical Continuum Emission in Active Galactic Nuclei: The Status of Accretion Disks. *PASP*, 111(755):1–30, Jan 1999. doi: 10.1086/316294.

[19] Ronald A. Remillard and Jeffrey E. McClintock. X-Ray Properties of Black-Hole Binaries. *ARA&A*, 44(1):49–92, Sep 2006. doi: 10.1146/annurev.astro. 44.051905.092532.

[20] M. A. Abramowicz, B. Czerny, J. P. Lasota, and E. Szuszkiewicz. Slim Accretion Disks. *ApJ*, 332:646, Sep 1988. doi: 10.1086/166683.

[21] A. Sadowski. Slim accretion disks around black holes. *arXiv e-prints*, art. arXiv:1108.0396, Aug 2011.

[22] Ken-ya Watarai, Tsunefumi Mizuno, and Shin Mineshige. Slim-Disk Model for Ultraluminous X-Ray Sources. *ApJ*, 549(1):L77–L80, Mar 2001. doi: 10. 1086/319125.

[23] Ken-Ya Watarai, Ken Ohsuga, Rohta Takahashi, and Jun Fukue. Geometrical Effect of Supercritical Accretion Flows: Observational Implications of Galactic Black-Hole Candidates and Ultraluminous X-Ray Sources. *PASJ*, 57:513–524, Jun 2005. doi: 10.1093/pasj/57.3.513.

[24] Feng Yuan and Ramesh Narayan. Hot Accretion Flows Around Black Holes. *ARA&A*, 52:529–588, Aug 2014. doi: 10.1146/annurev-astro-082812-141003.

[25] R. Narayan, I. Yi, and R. Mahadevan. Advection-dominated accretion model of Sagittarius A* and other accreting black holes. *A&AS*, 120:287–290, Dec 1996.

[26] Feng Yuan, Eliot Quataert, and Ramesh Narayan. Nonthermal Electrons in Radiatively Inefficient Accretion Flow Models of Sagittarius A*. *ApJ*, 598(1): 301–312, Nov 2003. doi: 10.1086/378716.

[27] F. Yuan. Advection-dominated Accretion: From Sgr A* to Other Low-luminosity AGNs. In L. C. Ho and J. W. Wang, editors, *The Central Engine of Active Galactic Nuclei*, volume 373 of *Astronomical Society of the Pacific Conference Series*, page 95, Oct 2007.

[28] Charles F. Gammie, Jonathan C. McKinney, and Gábor Tóth. HARM: A Numerical Scheme for General Relativistic Magnetohydrodynamics. *ApJ*, 589 (1):444–457, May 2003. doi: 10.1086/374594.

[29] S. A. Balbus and J. F. Hawley. A powerful local shear instability in weakly magnetized disks. I - Linear analysis. II - Nonlinear evolution. *ApJ*, 376: 214–233, July 1991. doi: 10.1086/170270.

[30] S. A. Balbus and J. F. Hawley. Instability, turbulence, and enhanced transport in accretion disks. *Reviews of Modern Physics*, 70:1–53, January 1998. doi: 10.1103/RevModPhys.70.1.

[31] E.P. Velikhov. Stability of an ideally conducting liquid flowing between rotating cylinders in a magnetic field. *Soviet Physics Journal of Experimental and Theoretical Physics*, 36(5), Nov 1959.

[32] Subrahmanyan Chandrasekhar. *Hydrodynamic and hydromagnetic stability.* 1961.

[33] S. A. Balbus and J. F. Hawley. *Numerical Simulations of MHD Turbulence in Accretion Disks*, volume 614, pages 329–348. 2003.

[34] R. P. Eatough, H. Falcke, R. Karuppusamy, K. J. Lee, D. J. Champion, E. F. Keane, G. Desvignes, D. H. F. M. Schnitzeler, L. G. Spitler, M. Kramer, B. Klein, C. Bassa, G. C. Bower, A. Brunthaler, I. Cognard, A. T. Deller, P. B. Demorest, P. C. C. Freire, A. Kraus, A. G. Lyne, A. Noutsos, B. Stappers, and N. Wex. A strong magnetic field around the supermassive black hole at the centre of the Galaxy. *Nature*, 501(7467):391–394, Sep 2013. doi: 10.1038/nature12499.

[35] M. Zamaninasab, E. Clausen-Brown, T. Savolainen, and A. Tchekhovskoy. Dynamically important magnetic fields near accreting supermassive black holes. *Nature*, 510(7503):126–128, Jun 2014. doi: 10.1038/nature13399.

[36] Philip Mocz and Xinyi Guo. Interpreting MAD within multiple accretion regimes. *MNRAS*, 447(2):1498–1503, Feb 2015. doi: 10.1093/mnras/stu2555.

[37] Kris Beckwith, John F. Hawley, and Julian H. Krolik. The Influence of Magnetic Field Geometry on the Evolution of Black Hole Accretion Flows: Similar Disks, Drastically Different Jets. *ApJ*, 678(2):1180–1199, May 2008. doi: 10.1086/533492.

[38] Jonathan C. McKinney and Roger D. Blandford. Stability of relativistic jets from rotating, accreting black holes via fully three-dimensional magnetohydrodynamic simulations. *MNRAS*, 394(1):L126–L130, Mar 2009. doi: 10.1111/j.1745-3933.2009.00625.x.

[39] R. Narayan, I. V. Igumenshchev, and M. A. Abramowicz. Magnetically Arrested Disk: an Energetically Efficient Accretion Flow. *PASJ*, 55:L69–L72, December 2003. doi: 10.1093/pasj/55.6.L69.

[40] J. C. McKinney, A. Tchekhovskoy, and R. D. Blandford. General relativistic magnetohydrodynamic simulations of magnetically choked accretion flows around black holes. *MNRAS*, 423:3083–3117, July 2012. doi: 10.1111/j.1365-2966.2012.21074.x.

[41] M. J. Avara, J. C. McKinney, and C. S. Reynolds. Efficiency of thin magnetically arrested discs around black holes. *MNRAS*, 462:636–648, October 2016. doi: 10.1093/mnras/stw1643.

[42] R. F. Elsner and F. K. Lamb. Accretion flows in the magnetospheres of VELA X-1, AO535 + 26 and HER X-1. *Nature*, 262:356–360, July 1976. doi: 10.1038/262356a0.

[43] R. F. Elsner and F. K. Lamb. Accretion by magnetic neutron stars. I - Magnetospheric structure and stability. *ApJ*, 215:897–913, August 1977. doi: 10.1086/155427.

[44] J. Arons and S.M. Lea. Accretion onto magnetized neutron stars - Structure and interchange instability of a model magnetosphere. *ApJ*, 207:914–936, August 1976. doi: 10.1086/154562.

[45] J. Arons and S. M. Lea. Accretion onto magnetized neutron stars - Normal mode analysis of the interchange instability at the magnetopause. *ApJ*, 210: 792–804, December 1976. doi: 10.1086/154888.

[46] M. Kaisig, T. Tajima, and R. V. E. Lovelace. Magnetic interchange instability of accretion disks. *ApJ*, 386:83–89, February 1992. doi: 10.1086/170994.

[47] S. H. Lubow and H. C. Spruit. Magnetic interchange instability in accretion disks. *ApJ*, 445:337–347, May 1995. doi: 10.1086/175698.

[48] H. C. Spruit, R. Stehle, and J. C. B. Papaloizou. Interchange instability in and accretion disc with a poloidal magnetic field. *MNRAS*, 275:1223–1231, August 1995. doi: 10.1093/mnras/275.4.1223.

[49] L.-X. Li and R. Narayan. Quasi-periodic Oscillations from Rayleigh-Taylor and Kelvin-Helmholtz Instability at a Disk-Magnetosphere Interface. *ApJ*, 601:414–427, January 2004. doi: 10.1086/380446.

[50] Roman V. Shcherbakov and Lei Huang. General relativistic polarized radiative transfer: building a dynamics-observations interface. *MNRAS*, 410(2):1052–1063, Jan 2011. doi: 10.1111/j.1365-2966.2010.17502.x.

[51] Roman V. Shcherbakov, Robert F. Penna, and Jonathan C. McKinney. Sagittarius A* Accretion Flow and Black Hole Parameters from General Relativistic Dynamical and Polarized Radiative Modeling. *ApJ*, 755(2):133, Aug 2012. doi: 10.1088/0004-637X/755/2/133.

[52] Roman V. Shcherbakov and Jonathan C. McKinney. Submillimeter Quasi-periodic Oscillations in Magnetically Choked Accretion Flow Models of SgrA*. *ApJ*, 774(2):L22, Sep 2013. doi: 10.1088/2041-8205/774/2/L22.

[53] Roman V. Shcherbakov. ASTRORAY: General relativistic polarized radiative transfer code, Jul 2014.

[54] José A. Font. Numerical Hydrodynamics and Magnetohydrodynamics in General Relativity. *Living Reviews in Relativity*, 11(1):7, Sep 2008. doi: 10.12942/lrr-2008-7.

[55] J. R. Wilson. Magnetohydrodynamics near a black hole. In *1st Marcel Grossmann Meeting on General Relativity*, volume 1, pages 393–413, Jan 1977.

[56] Peter Lax and Burton Wendroff. Systems of conservation laws. *Communications on Pure and Applied Mathematics*, 13(2):217–237, 1960. doi: 10.1002/cpa.3160130205. URL https://onlinelibrary.wiley.com/doi/abs/10.1002/cpa.3160130205.

[57] Randall J. Leveque. Nonlinear Conservation Laws and Finite Volume Methods. In O. Steiner and A. Gautschy, editors, *Saas-Fee Advanced Course 27: Computational Methods for Astrophysical Fluid Flow.*, page 1, Jan 1998.

[58] Scott C. Noble, Charles F. Gammie, Jonathan C. McKinney, and Luca Del Zanna. Primitive Variable Solvers for Conservative General Relativistic Magnetohydrodynamics. *ApJ*, 641(1):626–637, Apr 2006. doi: 10.1086/500349.

[59] A. Harten, P. Lax, and B. Leer. On upstream differencing and godunov-type schemes for hyperbolic conservation laws. *SIAM Review*, 25(1):35–61, 1983. doi: 10.1137/1025002. URL https://doi.org/10.1137/1025002.

[60] Gábor Tóth. The ∇· B=0 Constraint in Shock-Capturing Magnetohydrodynamics Codes. *Journal of Computational Physics*, 161(2):605–652, Jul 2000. doi: 10.1006/jcph.2000.6519.

[61] Anne Marie Porter and Rachel Ivie. Women in physics and astronomy, 2019. *American Institute of Physics Report*, March 2019. URL `https://www.aip.org/statistics/reports/women-physics-and-astronomy-2019`.

[62] J. M. Stone and T. Gardiner. Nonlinear evolution of the magnetohydrodynamic Rayleigh-Taylor instability. *Physics of Fluids*, 19(9):094104–094104, September 2007. doi: 10.1063/1.2767666.

[63] J. M. Stone and T. Gardiner. The Magnetic Rayleigh-Taylor Instability in Three Dimensions. *ApJ*, 671:1726–1735, December 2007. doi: 10.1086/523099.

[64] Y.-M. Wang and M. Nepveu. A numerical study of the nonlinear Rayleigh-Taylor instability, with application to accreting X-ray sources. *A&A*, 118: 267–274, February 1983.

[65] Y.-M. Wang, M. Nepveu, and J. A. Robertson. Further numerical studies of the Rayleigh-Taylor instability in the context of accreting X-ray sources. *A&A*, 135:66–76, June 1984.

[66] Y.-M. Wang and J. A. Robertson. Late stages of the Rayleigh-Taylor instability - A numerical study in the context of accreting neutron stars. *ApJ*, 299: 85–108, December 1985. doi: 10.1086/163684.

[67] H. C. Spruit and R. E. Taam. Mass transport in a neutron star magnetosphere. *A&A*, 229:475–493, March 1990.

[68] M. M. Romanova, A. K. Kulkarni, and R. V. E. Lovelace. Unstable Disk Accretion onto Magnetized Stars: First Global Three-dimensional Magnetohydrodynamic Simulations. *ApJ*, 673:L171, February 2008. doi: 10.1086/527298.

[69] A. K. Kulkarni and M. M. Romanova. Accretion to magnetized stars through the Rayleigh-Taylor instability: global 3D simulations. *MNRAS*, 386:673–687, May 2008. doi: 10.1111/j.1365-2966.2008.13094.x.

[70] M. M. Romanova, G. V. Ustyugova, A. V. Koldoba, and R. V. E. Lovelace. MRI-driven accretion on to magnetized stars: global 3D MHD simulations of magnetospheric and boundary layer regimes. *MNRAS*, 421:63–77, March 2012. doi: 10.1111/j.1365-2966.2011.20055.x.

[71] A. A. Blinova, M. M. Romanova, and R. V. E. Lovelace. Boundary between stable and unstable regimes of accretion. Ordered and chaotic unstable regimes. *MNRAS*, 459:2354–2369, July 2016. doi: 10.1093/mnras/stw786.

[72] I. V. Igumenshchev. Magnetically Arrested Disks and the Origin of Poynting Jets: A Numerical Study. *ApJ*, 677:317-326, April 2008. doi: 10.1086/529025.

[73] A. Tchekhovskoy, J. C. McKinney, and R. Narayan. General Relativistic Modeling of Magnetized Jets from Accreting Black Holes. In *Journal of Physics Conference Series*, volume 372 of *Journal of Physics Conference Series*, page 012040, July 2012. doi: 10.1088/1742-6596/372/1/012040.

[74] S. Hirose, J. H. Krolik, J.-P. De Villiers, and J. F. Hawley. Magnetically Driven Accretion Flows in the Kerr Metric. II. Structure of the Magnetic Field. *ApJ*, 606:1083–1097, May 2004. doi: 10.1086/383184.

[75] A. K. Kulkarni, R. F. Penna, R. V. Shcherbakov, J. F. Steiner, R. Narayan, A. Sä Dowski, Y. Zhu, J. E. McClintock, S. W. Davis, and J. C. McKinney. Measuring black hole spin by the continuum-fitting method: effect of deviations from the Novikov-Thorne disc model. *MNRAS*, 414:1183–1194, June 2011. doi: 10.1111/j.1365-2966.2011.18446.x.

[76] X. Guan and C. F. Gammie. The Turbulent Magnetic Prandtl Number of MHD Turbulence in Disks. *ApJ*, 697:1901–1906, June 2009. doi: 10.1088/0004-637X/697/2/1901.

[77] Event Horizon Telescope Collaboration, Kazunori Akiyama, Antxon Alberdi, Walter Alef, Keiichi Asada, Rebecca Azulay, Anne-Kathrin Baczko, David Ball, Mislav Baloković, and John Barrett. First M87 Event Horizon Telescope Results. I. The Shadow of the Supermassive Black Hole. *ApJ*, 875(1):L1, Apr 2019. doi: 10.3847/2041-8213/ab0ec7.

[78] Event Horizon Telescope Collaboration, Kazunori Akiyama, Antxon Alberdi, Walter Alef, Keiichi Asada, Rebecca Azulay, Anne-Kathrin Baczko, David Ball, Mislav Baloković, and John Barrett. First M87 Event Horizon Telescope Results. II. Array and Instrumentation. *ApJ*, 875(1):L2, Apr 2019. doi: 10.3847/2041-8213/ab0c96.

[79] Event Horizon Telescope Collaboration, Kazunori Akiyama, Antxon Alberdi, Walter Alef, Keiichi Asada, Rebecca Azulay, Anne-Kathrin Baczko, David Ball, Mislav Baloković, and John Barrett. First M87 Event Horizon Telescope Results. III. Data Processing and Calibration. *ApJ*, 875(1):L3, Apr 2019. doi: 10.3847/2041-8213/ab0c57.

[80] Event Horizon Telescope Collaboration, Kazunori Akiyama, Antxon Alberdi, Walter Alef, Keiichi Asada, Rebecca Azulay, Anne-Kathrin Baczko, David Ball, Mislav Baloković, and John Barrett. First M87 Event Horizon Telescope Results. IV. Imaging the Central Supermassive Black Hole. *ApJ*, 875(1):L4, Apr 2019. doi: 10.3847/2041-8213/ab0e85.

[81] Event Horizon Telescope Collaboration, Kazunori Akiyama, Antxon Alberdi, Walter Alef, Keiichi Asada, Rebecca Azulay, Anne-Kathrin Baczko, David Ball, Mislav Baloković, and John Barrett. First M87 Event Horizon Telescope Results. V. Physical Origin of the Asymmetric Ring. *ApJ*, 875(1):L5, Apr 2019. doi: 10.3847/2041-8213/ab0f43.

[82] Event Horizon Telescope Collaboration, Kazunori Akiyama, Antxon Alberdi, Walter Alef, Keiichi Asada, Rebecca Azulay, Anne-Kathrin Baczko, David Ball, Mislav Baloković, and John Barrett. First M87 Event Horizon Telescope Results. VI. The Shadow and Mass of the Central Black Hole. *ApJ*, 875(1): L6, Apr 2019. doi: 10.3847/2041-8213/ab1141.

[83] Monika Mościbrodzka, Heino Falcke, Hotaka Shiokawa, and Charles F. Gammie. Observational appearance of inefficient accretion flows and jets in 3D GRMHD simulations: Application to Sagittarius A*. *A&A*, 570:A7, Oct 2014. doi: 10.1051/0004-6361/201424358.

[84] Monika Mościbrodzka, Heino Falcke, and Hotaka Shiokawa. General relativistic magnetohydrodynamical simulations of the jet in M 87. *A&A*, 586:A38, Feb 2016. doi: 10.1051/0004-6361/201526630.

[85] Andrew Chael, Ramesh Narayan, and Michael D. Johnson. Two-temperature, Magnetically Arrested Disc simulations of the jet from the supermassive black hole in M87. *MNRAS*, 486(2):2873–2895, Jun 2019. doi: 10.1093/mnras/stz988.

[86] Roman Gold, Jonathan C. McKinney, Michael D. Johnson, and Sheperd S. Doeleman. Probing the Magnetic Field Structure in Sgr A* on Black Hole Horizon Scales with Polarized Radiative Transfer Simulations. *ApJ*, 837(2): 180, Mar 2017. doi: 10.3847/1538-4357/aa6193.

[87] R. Fraga-Encinas, M. Mościbrodzka, C. Brinkerink, and H. Falcke. Probing spacetime around Sagittarius A* using modeled VLBI closure phases. *A&A*, 588:A57, Apr 2016. doi: 10.1051/0004-6361/201527599.

[88] Hung-Yi Pu and Avery E. Broderick. Probing the Innermost Accretion Flow Geometry of Sgr A* with Event Horizon Telescope. *ApJ*, 863(2):148, Aug 2018. doi: 10.3847/1538-4357/aad086.

[89] Yu. E. Lyubarskii. Flicker noise in accretion discs. *MNRAS*, 292(3):679–685, Dec 1997. doi: 10.1093/mnras/292.3.679.

[90] Jongho Park and Sascha Trippe. The Long-term Centimeter Variability of Active Galactic Nuclei: A New Relation between Variability Timescale and Accretion Rate. *ApJ*, 834(2):157, Jan 2017. doi: 10.3847/1538-4357/834/2/157.

[91] H. E. Bignall, S. Croft, T. Hovatta, J. Y. Koay, J. Lazio, J. P. Macquart, and C. Reynolds. Time domain studies of Active Galactic Nuclei with the Square Kilometre Array. In *Advancing Astrophysics with the Square Kilometre Array (AASKA14)*, page 58, Apr 2015.

[92] Seok Jae Park and Ethan T. Vishniac. The Variability of Active Galactic Nuclei and the Radial Transport of Vertical Magnetic Flux. *ApJ*, 471:158, Nov 1996. doi: 10.1086/177959.

[93] Joshua E. Goldston, Eliot Quataert, and Igor V. Igumenshchev. Synchrotron Radiation from Radiatively Inefficient Accretion Flow Simulations: Applications to Sagittarius A*. *ApJ*, 621(2):785–792, Mar 2005. doi: 10.1086/427741.

[94] Jason Dexter and Mitchell C. Begelman. Extreme AGN variability: evidence of magnetically elevated accretion? *MNRAS*, 483(1):L17–L21, Feb 2019. doi: 10.1093/mnrasl/sly213.

[95] Denise Gabuzda. Astrophysics: The MAD world of black holes. *Nature*, 510 (7503):42–43, Jun 2014. doi: 10.1038/510042a.

[96] Chi-kwan Chan, Dimitrios Psaltis, Feryal Özel, Lia Medeiros, Daniel Marrone, Aleksander Saowski, and Ramesh Narayan. Fast Variability and Millimeter/IR Flares in GRMHD Models of Sgr A* from Strong-field Gravitational Lensing. *ApJ*, 812(2):103, Oct 2015. doi: 10.1088/0004-637X/812/2/103.

[97] Lia Medeiros, Chi-kwan Chan, Feryal Özel, Dimitrios Psaltis, Junhan Kim, Daniel P. Marrone, and Aleksander Saowski. GRMHD Simulations of Visibility Amplitude Variability for Event Horizon Telescope Images of Sgr A*. *ApJ*, 856(2):163, Apr 2018. doi: 10.3847/1538-4357/aab204.

[98] Auna L. Moser and Paul M. Bellan. Magnetic reconnection from a multiscale instability cascade. *Nature*, 482(7385):379–381, Feb 2012. doi: 10.1038/nature10827.

[99] Kyle A. Baldwin, Matthew M. Scase, and Richard J. A. Hill. The Inhibition of the Rayleigh-Taylor Instability by Rotation. *Scientific Reports*, 5:11706, Jul 2015. doi: 10.1038/srep11706.

[100] Andrew Hillier. The magnetic Rayleigh-Taylor instability in solar prominences. *Reviews of Modern Plasma Physics*, 2(1):1, Dec 2018. doi: 10.1007/s41614-017-0013-2.

[101] Sudheer K. Mishra, Talwinder Singh, P. Kayshap, and A. K. Srivastava. Evolution of Magnetic Rayleigh-Taylor Instability into the Outer Solar Corona and Low Interplanetary Space. *ApJ*, 856(1):86, Mar 2018. doi: 10.3847/1538-4357/aaae03.

[102] J. Jeff Hester, James M. Stone, Paul A. Scowen, Byung-Il Jun, III Gallagher, John S., Michael L. Norman, Gilda E. Ballester, Christopher J. Burrows, Stefano Casertano, and John T. Clarke. WFPC2 Studies of the Crab Nebula. III. Magnetic Rayleigh-Taylor Instabilities and the Origin of the Filaments. *ApJ*, 456:225, Jan 1996. doi: 10.1086/176643.

[103] Prateek Sharma, Eliot Quataert, Gregory W. Hammett, and James M. Stone. Electron Heating in Hot Accretion Flows. *ApJ*, 667(2):714–723, Oct 2007. doi: 10.1086/520800.

[104] Avery E. Broderick and Abraham Loeb. Imaging bright-spots in the accretion flow near the black hole horizon of Sgr A*. *MNRAS*, 363(2):353–362, Oct 2005. doi: 10.1111/j.1365-2966.2005.09458.x.

[105] Avery E. Broderick and Abraham Loeb. Imaging optically-thin hotspots near the black hole horizon of Sgr A* at radio and near-infrared wavelengths. *MNRAS*, 367(3):905–916, Apr 2006. doi: 10.1111/j.1365-2966.2006.10152.x.

[106] Sheperd S. Doeleman, Vincent L. Fish, Avery E. Broderick, Abraham Loeb, and Alan E. E. Rogers. Detecting Flaring Structures in Sagittarius A* with High-Frequency VLBI. *ApJ*, 695(1):59–74, Apr 2009. doi: 10.1088/0004-637X/695/1/59.

[107] Chi-kwan Chan, Siming Liu, Christopher L. Fryer, Dimitrios Psaltis, Feryal Özel, Gabriel Rockefeller, and Fulvio Melia. MHD Simulations of Accretion onto Sgr A*: Quiescent Fluctuations, Outbursts, and Quasiperiodicity. *ApJ*, 701(1):521–534, Aug 2009. doi: 10.1088/0004-637X/701/1/521.

[108] Toni A Campbell and David E Campbell. Faculty/student mentor program: Effects on academic performance and retention. *Research in higher education*, 38(6):727–742, 1997.

[109] William D. Mangold, Luann G. Bean, Douglas J. Adams, William A. Schwab, and Scott M. Lynch. Who goes who stays: An assessment of the effect of a freshman mentoring and unit registration program on college persistence. *Journal of College Student Retention: Research, Theory & Practice*, 4(2):95–122, August 2002. doi: 10.2190/cvet-tmdm-cte4-afe3. URL `https://doi.org/10.2190/cvet-tmdm-cte4-afe3`.

[110] Amaury Nora and Gloria Crisp. Mentoring students: Conceptualizing and validating the multi-dimensions of a support system. *Journal of College Student Retention: Research, Theory & Practice*, 9(3):337–356, November 2007. doi: 10.2190/cs.9.3.e. URL `https://doi.org/10.2190/cs.9.3.e`.

[111] Tara C. Dennehy and Nilanjana Dasgupta. Female peer mentors early in college increase women's positive academic experiences and retention in engineering. *Proceedings of the National Academy of Sciences*, 114(23):5964–5969, May 2017. doi: 10.1073/pnas.1613117114. URL `https://doi.org/10.1073/pnas.1613117114`.

[112] Tammy D. Allen, Stacy E. McManus, and Joyce E.A. Russell. Newcomer socialization and stress: Formal peer relationships as a source of support. *Journal of Vocational Behavior*, 54(3):453 – 470, 1999. ISSN 0001-8791. doi: https://doi.org/10.1006/jvbe.1998.1674. URL `http://www.sciencedirect.com/science/article/pii/S0001879198916748`.

[113] Andrew Miller. *Mentoring Students and Young People: A Handbook of Effective Practice*. Falmer Press, 2002. ISBN 0749435437. URL `https:`

//www.amazon.com/Mentoring-Students-Young-People-Effective/
dp/0749435437?SubscriptionId=AKIAIOBINVZYXZQZ2U3A&tag=
chimbori05-20&linkCode=xm2&camp=2025&creative=165953&
creativeASIN=0749435437.

[114] Paula Wilcox, Sandra Winn, and Marylynn Fyvie-Gauld. 'it was nothing to do with the university, it was just the people': the role of social support in the first-year experience of higher education. *Studies in Higher Education*, 30 (6):707–722, December 2005. doi: 10.1080/03075070500340036. URL `https://doi.org/10.1080/03075070500340036`.

[115] Jaime L. Shook and Jennifer R. Keup. The benefits of peer leader programs: An overview from the literature. *New Directions for Higher Education*, 2012 (157):5–16, March 2012. doi: 10.1002/he.20002. URL `https://doi.org/10.1002/he.20002`.

[116] Jane G. Stout, Tiffany A. Ito, Noah D. Finkelstein, and Steven J. Pollock. How a gender gap in belonging contributes to the gender gap in physics participation. AIP, 2013. doi: 10.1063/1.4789737. URL `https://doi.org/10.1063/1.4789737`.

[117] Karyn L. Lewis, Jane G. Stout, Steven J. Pollock, Noah D. Finkelstein, and Tiffany A. Ito. Fitting in or opting out: A review of key social-psychological factors influencing a sense of belonging for women in physics. *Physical Review Physics Education Research*, 12(2), August 2016. doi: 10.1103/physrevphyseducres.12.020110. URL `https://doi.org/10.1103/physrevphyseducres.12.020110`.

[118] Melinda McCormick, Ramon S. Barthelemy, and Charles Henderson. Women's persistence into graduate astronomy programs: The roles of support, interest, and capital. *Journal of Women and Minorities in Science and Engineering*, 20(4):317–340, 2014. doi: 10.1615/jwomenminorscieneng.2014009829. URL `https://doi.org/10.1615/jwomenminorscieneng.2014009829`.

[119] Elaine Seymour and Nancy M Hewitt. *Talking About Leaving: Why Undergraduates Leave The Sciences*. Westview Press, 1996. ISBN 0813389267. URL `https://www.amazon.com/Talking-About-Leaving-Undergraduates-Sciences/dp/0813389267?SubscriptionId=AKIAIOBINVZYXZQZ2U3A&tag=chimbori05-20&linkCode=xm2&camp=2025&creative=165953&creativeASIN=0813389267`.

[120] Barbara L. Whitten, Suzanne R. Foster, Margaret L. Duncombe, Patricia E. Allen, Paula Heron, Laura McCullough, Kimberly A. Shaw, Beverley A. P. Taylor, and Heather M. Zorn. WHAT WORKS? INCREASING THE PARTICIPATION OF WOMEN IN UNDERGRADUATE PHYSICS. *Journal of Women and Minorities in Science and Engineering*, 9(3-4):20, 2003. doi: 10.1615/jwomenminorscieneng.v9.i34.30. URL `https://doi.org/10.1615/jwomenminorscieneng.v9.i34.30`.

[121] Maryann Jacobi. Mentoring and undergraduate academic success: A literature review. *Review of Educational Research*, 61(4):505–532, December 1991. doi: 10.3102/00346543061004505. URL `https://doi.org/10.3102/00346543061004505`.

[122] Elizabeth A. Bennion. The importance of peer mentoring for facilitating professional and personal development. *PS: Political Science & Politics*, 37(1):111113, 2004. doi: 10.1017/S1049096504003841.

[123] Anna M. Zaniewski and Daniel Reinholz. Increasing STEM success: a near-peer mentoring program in the physical sciences. *International Journal of STEM Education*, 3(1), August 2016. doi: 10.1186/s40594-016-0043-2. URL `https://doi.org/10.1186/s40594-016-0043-2`.

[124] Badr F. Albanna, Joel C. Corbo, Dimitri R. Dounas-Frazer, Angela Little, and Anna M. Zaniewski. Building classroom and organizational structure around positive cultural values. AIP, 2013. doi: 10.1063/1.4789638. URL `https://doi.org/10.1063/1.4789638`.

[125] Gloria Crisp and Irene Cruz. Mentoring college students: A critical review of the literature between 1990 and 2007. *Research in Higher Education*, 50(6):525–545, 2009. ISSN 03610365, 1573188X. URL `http://www.jstor.org/stable/29782942`.

[126] Susan Gershenfeld. A review of undergraduate mentoring programs. *Review of Educational Research*, 84(3):365–391, September 2014. doi: 10.3102/0034654313520512. URL `https://doi.org/10.3102/0034654313520512`.

[127] Nilanjana Dasgupta. Ingroup experts and peers as social vaccines who inoculate the self-concept: The stereotype inoculation model. *Psychological Inquiry*, 22(4):231–246, October 2011. doi: 10.1080/1047840x.2011.607313. URL `https://doi.org/10.1080/1047840x.2011.607313`.

[128] Samantha Sinclair, Rickard Carlsson, and Fredrik Björklund. The role of friends in career compromise: Same-gender friendship intensifies gender differences in educational choice. *Journal of Vocational Behavior*, 84(2):109–118, April 2014. doi: 10.1016/j.jvb.2013.12.007. URL `https://doi.org/10.1016/j.jvb.2013.12.007`.

[129] Norman H. Cohen and Michael W. Galbraith. Mentoring in the learning society. *New Directions for Adult and Continuing Education*, 1995(66):5–14, 1995. doi: 10.1002/ace.36719956603. URL `https://doi.org/10.1002/ace.36719956603`.

[130] Robert J. Cramer and Steven Prentice-Dunn. Caring for the whole person: Guidelines for advancing undergraduate mentorship. *College Student Journal*, 41(4):771 – 778, 2007. ISSN 01463934. URL `http://search.ebscohost.com/login.aspx?direct=true&db=s3h&AN=28351173&site=ehost-live`.

[131] Bonita London, Lisa Rosenthal, Sheri R. Levy, and Marci Lobel. The influences of perceived identity compatibility and social support on women in nontraditional fields during the college transition. *Basic and Applied Social Psychology*, 33(4):304–321, October 2011. doi: 10.1080/01973533.2011.614166. URL https://doi.org/10.1080/01973533.2011.614166.

[132] Geoff Potvin and Zahra Hazari. The development and measurement of identity across the physical sciences. In *2013 Physics Education Research Conference Proceedings*. American Association of Physics Teachers, February 2014. doi: 10.1119/perc.2013.pr.058. URL https://doi.org/10.1119/perc.2013.pr.058.

[133] Gina Quan. *Becoming a Physicist: How Identities and Practices Shape Physics Trajectories*. PhD thesis, 2017. URL http://drum.lib.umd.edu/handle/1903/19900.

[134] Frances Gunn, Seung Hwan (Mark) Lee, and Madelyn Steed. Student perceptions of benefits and challenges of peer mentoring programs: Divergent perspectives from mentors and mentees. *Marketing Education Review*, 27(1):15–26, 2017. doi: 10.1080/10528008.2016.1255560. URL https://doi.org/10.1080/10528008.2016.1255560.

[135] Jennifer M. Good, Glennelle Halpin, and Gerald Halpin. A promising prospect for minority retention: Students becoming peer mentors. *The Journal of Negro Education*, 69(4):375, 2000. doi: 10.2307/2696252. URL https://doi.org/10.2307/2696252.

[136] Tracy L. Skipper and Jennifer R. Keup. The perceived impact of peer leadership experiences on college academic performance. *Journal of Student Affairs Research and Practice*, 54(1):95–108, August 2016. doi: 10.1080/19496591.2016.1204309. URL https://doi.org/10.1080/19496591.2016.1204309.

[137] Susan Beltman and Marcel Schaeben. Institution-wide peer mentoring: Benefits for mentors. *The International Journal of the First Year in Higher Education*, 3(2), July 2012. doi: 10.5204/intjfyhe.v3i2.124. URL https://doi.org/10.5204/intjfyhe.v3i2.124.

[138] Anna M. Zaniewski. personal communication, August 2017.

[139] Hannah Shamloo and Anna Zaniewski. Designing a near-peer mentoring program for science majors, December 2017.

[140] Kendra M. Hall, Roni Jo Draper, Leigh K. Smith, and Robert V. Bullough. More than a place to teach: exploring the perceptions of the roles and responsibilities of mentor teachers. *Mentoring & Tutoring: Partnership in Learning*, 16(3):328–345, August 2008. doi: 10.1080/13611260802231708. URL https://doi.org/10.1080/13611260802231708.

[141] David Ernst, Eric Hooper, Catherine Mader, Christine Pfund, Alejandro Rodriguez-Wong, and Chandra Turpen. *Physics Research Mentor Training Seminar.* American Physical Society, 2011.